CHALMERS

BioRID II final report

JOHAN DAVIDSSON

Crash Safety Division
Department of Machine and Vehicle Design
CHALMERS UNIVERSITY OF TECHNOLOGY
Göteborg, Sweden 1999

Report December 30, 1999

Summary

There is currently no established method for performance testing of seat systems in rear-end collisions. The most important component for such a test method is a crash test dummy. Several investigators have noted limitations of the most commonly used dummy in rear impact testing, the Hybrid III. Its neck and torso is too stiff. Other limitations are inappropriate back curvature, pelvic-femur joint characteristics and the limited use ability of the Hybrid III in out-of-position testing.

The objectives of this study have been to develop dummy prototypes for low speed rear-end collision testing. These dummy prototypes have new articulated spines, new muscle substitutes and a new torsos. The prototypes are equipped with Hybrid III legs, arms, modified Hybrid III heads and pelvises.

This report describes the development of these dummy prototypes. The influence of spine stiffness, torso stiffness, neck muscle substitutes characteristics and clothing on dummy prototype kinematics are also reported on. This report also describes handling, assembly, adjustments and calibration of the final dummy model.

Table of Contents

B31 Damper body

B32 Damper paddle wheel

B33 Damper cover

B34 Damper washer

B35 Arm attachment reinforcement, schematic

B36 Arm-torso attachment reinforcement, left

B37 Arm-torso attachment reinforcement, right

B38 Arm attachment

B39 Abdomen attachment

B40 Spine-torso interface, left and right

B41 Spine-torsion pin

B42 Shoulder yoke

B43 Pelvis interface abdomen attachment

B44 Pelvis position indicator attachment

B45 Pelvis position indicator

B46 Pelvis position indicator relative to the H-point

B47 T1 position indicator

B48 H-point position attachment

B49 Neck load cell modification

B50 Head modifications

B51 Spine box

B52 Calibration rig

B53 Calibration rig attachment

List of Tables

List of Figures

Acknowledgements

This project was part of the Swedish Vehicle Research Program and was administrated by NUTEK, Sweden. The project was carried out in co-operation with Autoliv Development AB, Volvo Car Corporation and Saab Automobile AB. Dummy prototype parts were manufactured by the department, Applied Safety Technologies Corporation Inc., Autoliv Sweden AB and BoMekansika AB.

I thank all those who have helped me in writing this report, especially:

Anders Flogård, Technician at Crash Safety Division, for his valuable ideas, engineering knowledge, practical skills and enthusiasm.

Dr. Per Lövsund, Professor at Crash safety Division, my advisor, for advise his encouragement.

Dr. Mats Svensson, Assistant Professor, my advisor, for his help and advice in the art of biomechanics and crash test dummies for rear impacts.

Ms. Astrid Linder, my colleague, for valuable criticism.

Mats Nillius, Hans Sjöberg and Ulrika Krave for their help in the test laboratory.

1 The design and performance of the BioRID prototypes

1.1 Introduction

Currently there is no adequate tool for testing the performance of car seats and head restraints in rear end collisions. The best available dummy is the Hybrid III. Its neck and spinal structure is stiff and unlikely to interact with the seat back in the as would that of a human.

Seemann et al. (1986) found the Hybrid III neck far too stiff to respond in a human-like manner in the sagittal plane. Deng (1989) reported that results from a mathematical model of the Hybrid III neck indicated that the neck has a torque response similar to that of the human neck but has a higher shear response. Foret-Bruno et al. (1991) compared the Hybrid III dummy with a cadaver in simulated rear impact using a head restraint closely fitted to the head, to minimize the relative movement between head and torso. The cadaver showed no sign of injury. However, very large shear forces at occipital level were registered in the Hybrid III test. The authors concluded that the human head can move relative to the torso with very limited stresses to the neck, but this is not the case for the dummy.

Svensson and Lövsund (1992) developed and validated a Rear Impact Dummy-neck (RID-neck) that can be used on the Hybrid III dummy. The new neck was designed for rear-end collision testing at low impact-velocities. It consisted of seven cervical and two thoracic vertebrae. The RID-neck was validated using data from a test series with volunteers (Tarriere and Sapin, 1969) after a study by Tisserand and Wisner (1966). These validation data only included the angular displacement of the head relative to the torso but did not allow for validation of the initial rearward translation motion of the head.

Thunnissen et al. (1996) developed a new rear impact dummy neck, the TRID-neck (TNO Rear Impact Dummy-neck) based partly on the RID-neck design. The TRID was subjected to a more extensive validation, but which was still restricted to the angular displacement between head and torso. The number of pin joints had been reduced from nine (RID) to seven (TRID) and efforts had been made to achieve adequate repeatability and reproducibility. The dynamic responses of these necks appear to be very similar.

The aim of this study is to develop a 50%-ile crash test dummy prototypes for evaluation of the performance of car-seat systems in rear-end collision testing. The dummy prototypes have been given the name Biofidelic Rear Impact Dummy (BioRID) P1, P2 and P3. They have new articulated spines, new muscle substitutes, and new flexible torsos and redesigned Hybrid III arm attachments and pelvises.

This chapter attempts to address three issues:
- Describe the general designs of three versions of BioRID prototypes.
- Describe the rationales behind the design changes introduced in BioRID P2 and BioRID P3.
- Propose improvements for the next generation of BioRID prototypes.

1.2 General Dummy Designs

New dummy prototypes for rear-end collision testing at low velocity changes were developed to resemble the human being in seated posture and to replicate the human motion in a rear end impact (Figure 3, Figure 9 and Figure 16).

Spine

The BioRID spine consists of the same number of vertebrae as that of a human, i.e. 7 cervical, 12 thoracic and 5 lumbar vertebrae. The head and the top cervical vertebra is connected to each other by means of occipital interface. The occipital interface is rigidly mounted to a modified version of Denton type 2564 or 4037 Eng Hybrid III upper neck load cell. The top cervical vertebra and the occipital interface have special designs that allow the head to be horizontal while maintaining the same joint characteristics as the rest of the neck joints. The top thoracic vertebra is a hybrid; its upper side designed like a cervical vertebra and the bottom surface as a thoracic vertebra. The T1 upper face is also tilted rearward relative to the lower face. The upper surface of the top lumbar vertebrae matches the thoracic vertebra design and is tilted slightly rearward. The bottom lumbar vertebra is connected to a pelvis interface which, in turn, is mounted to the pelvis.

The BioRID P1 vertebrae are made of aluminum and the BioRID P2/I and P3/II are made in durable plastic (Acetal). The vertebrae are connected with pin joints that only allow for angular motion in the sagittal plane. All occipital interfaces and pelvis interfaces are made of aluminum. The cervical, thoracic and lumbar vertebrae are of the same height: 17.5 mm, 26.5 mm and 30.5 mm respectively (Figure 1).

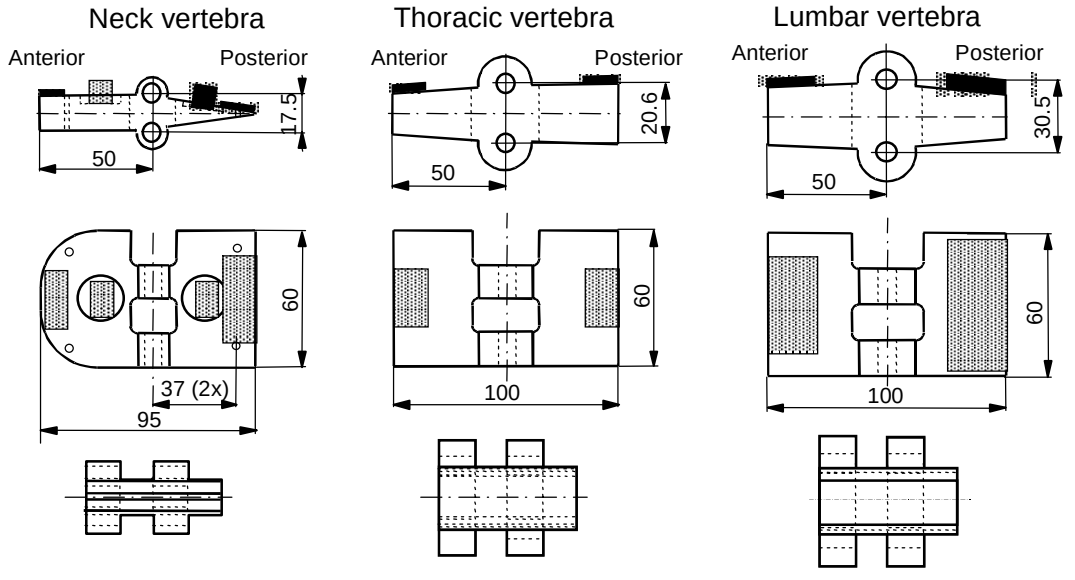

Figure 1. Schematic of the BioRID vertebrae with polyurethane (blocks, side, top and frontal view) [mm].

In the inter-spaces between all vertebrae, there are blocks of polyurethane rubber glued to the nearest inferior vertebra (Figure 1). Two blocks are in the neck: the first contributes to the overall joint characteristics while the second is activated only when

the spine is hyper-extended or hyper-flexed (Figure 1). The thoracic and lumbar spine are only equipped with blocks of the latter type. In the thoracic and lumbar spine, the steel pin joints constitute linear torsion springs (Figure 2). The ends of the pins are connected on each side respectively to the superior and to the inferior pin by means of steel washers (BioRID P1 Figure 3, and BioRID P2 and P3 Figure 2). The pin diameter and size of rubber blocks for the thoracic spine was different among the dummies, see Table 2 and Table 4.

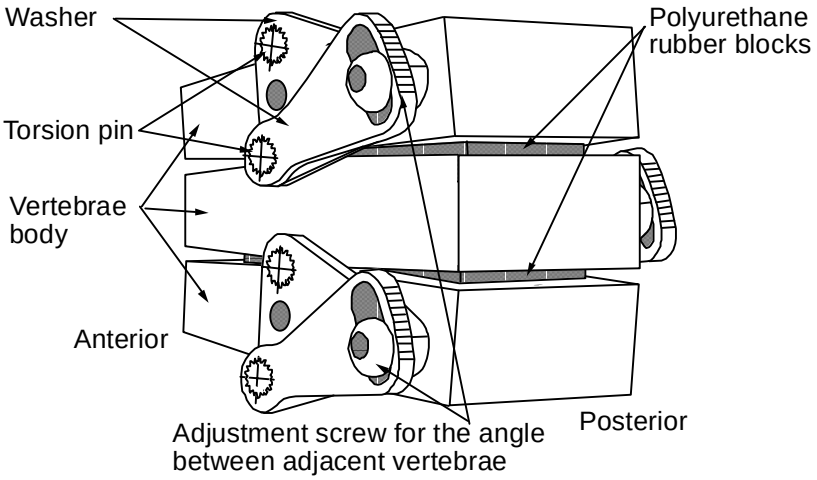

Figure 2. Schematic of three thoracic vertebrae with torsion springs/pin-joints, washers (oblique rear view).

For all BioRID prototypes, the cervical vertebrae and the occipital interface, thoracic and lumbar vertebrae have the same angular range of motion relative to the nearest inferior vertebra (Table 2). The chosen range of motion of the lumbar, thoracic and cervical spine were based on data from the literature and adjusted for seated posture (Andersson et al. 1979).

Table 1. Comparison between BioRID vertebrae range of motion and literature data [deg].

Dummy/ Reference:	BioRID	White & Panjabi, 1978	Kampanj, 1974*		Moffatt et al., 1979	Dvorak et al., 1988	Dvorak et al., 1991	Snyder et al., 1975*
Direction:	Ext./Flex.	Total RoM	Ext./Flex.	Total RoM	Total RoM	Total RoM	Total RoM	Ext./Flex.
Cervical	11.5/4.5	8-17 (12.3)	-	-	13-21 (16.5)	12-23 (18.2)	-	10.0/6.9
Thoracic	3.0/3.0	4-12 (6.3)	2.1/3.8	-	-	-	-	-
Lumbar	10.0/5.0	12-20 (15.6)	6.0/8.0	11-24 (16.6)	-	-	12-18 (15.3)	-

* The body segment range of motion in extension and in flexion for the human in standing posture evenly distributed on the joints included in the particular segment (cervical 8, thoracic 12 and lumbar 5 joints).

Schneider et al. (1983) established a set of co-ordinates for the joint centers of the human bones, center of gravity of various body parts of an average midsize male in seated posture. The spinal joint center co-ordinates could relatively precise be represented by two arches, one arc for the thoracic kyphosis and one arc for the neck, and one line for the lumbar spine. The BioRID spine consists therefore of only three major types of vertebrae.

Neck muscle substitute design

In order to better replicate the human head and neck retraction motion (head lag), and thus more precisely injury risk, the new necks are equipped with muscle substitutes. In all dummy prototypes, these consist of cables originating from the head, in the front and in the back of the occipital joint, guided through the cervical vertebrae and terminating at either T1 or T3. At T1 and T3 the cable load is transferred to either a spring or a damper and a spring in parallel with a damper.

Torso

The torso prototypes consist of chest and abdomen, and are made in different silicon rubber materials. These torsos were fitted with different arm attachment designs, different water bladder designs, different sizes and number of cuts and different spine-torso interfaces.

In all three BioRID prototypes the torsos resembles a seated 50% male (Schneider et al. 1983) and there is a curved rectangular containment inside the torso to contain the spine. Between the back of the vertebrae and the rubber torso is a Teflon foil/sheets of foam to reduce friction between vertebrae and torso. Steel tubes with a diameter of 10 mm connect the rubber torso with the spine (Figure 3, Figure 9, and Figure 16). The bottom of the rubber torso is connected to the pelvis interface that in turn is mounted to the pelvis.

Pelvis redesign

The BioRID P1 are fitted a modified Hybrid III pedestrian pelvis, the BioRID P2 and P3 are fitted a modified Hybrid III pelvis. The P2/I and P3 pelvis mass was reduced from 9.3 kg to 8.8 kg. In all prototypes, the original Hybrid III pelvis anterior-superior iliac spine height was decreased to conform with the modifications of the AATD (Schneider et al. 1992) and agree with the average male pelvis (Reynolds et al. 1981). The original pelvis front flesh is removed to allow the abdomen to bulge forward. For the BioRID P2/I and P3, the pelvis flesh is modified to reduce femur joint flexion/extension resistance. This was achieved by enlarging the holes in the flesh that accommodate the femur bones.

Head, legs and arms

The BioRID P1 and P2/I are equipped with standard Hybrid III legs, arms and heads. The P3 is fitted with a modified Hybrid III head and with standard Hybrid III legs and arms.

Sitting posture

The normal BioRID seating posture resembles that of an average human in a standard US bucket car seat from the middle of 1980 (Schneider et al. 1983).

Clothing

The BioRID prototype was either dressed in shirts and pants made in cotton clothing, double layer of shirts and pants made in Lycra, or seated on two layers of Lycra (Table 2 and Table 4). The Lycra dress/sheets were introduced to mimic the slack observed between the human bone and skin as well as to mimic the slip observed to take place between the human skin and clothing in a rear impact.

Mass properties

The mass properties were essentially the same for all prototypes as that of the BioRID I and BioRID II and are to be found in chapter 12.

1.3 BioRID P1

Materials and method

DUMMY DESIGN - The first BioRID prototype was quite different from its successor. The following parts were either different in design or was made in materials with different properties from that of the successor, the BioRID P2:

- The thoracic and lumbar spine torsion pin diameter was 8 mm.
- The vertebrae were made in aluminum.
- Torso was made in SI- silicon.
- The number of spine-torso interface pins was in total 30.
- The upper part of the torso was cut at four levels.
- The neck muscle substitutes were connected to springs only (no damper).
- The dummy was dressed in shirt and pants made in cotton.
- The dummy was fitted a modified Hybrid III pedestrian pelvis.

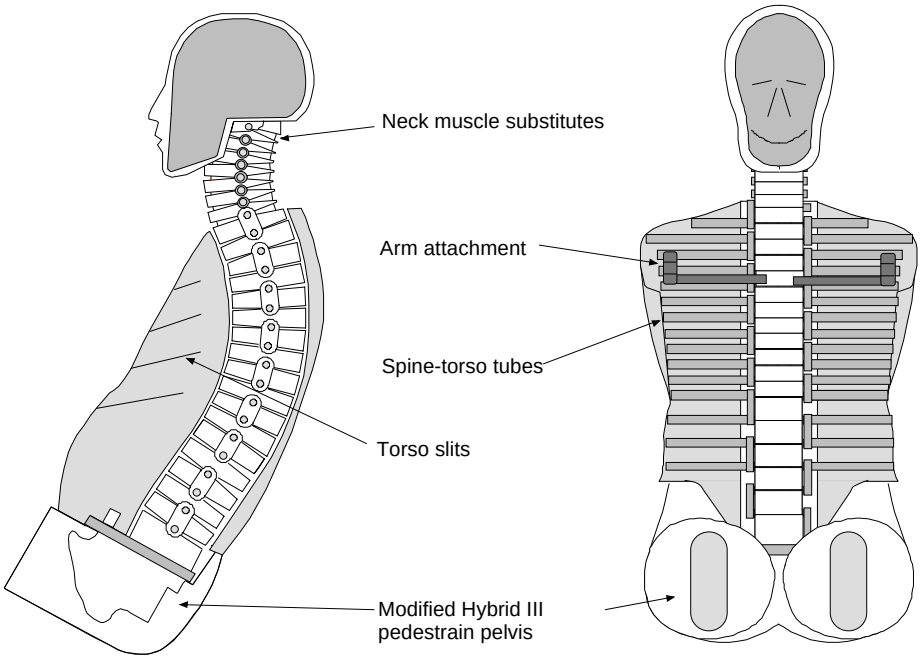

Figure 3. X-ray view of parts of the BioRID P1.

VALIDATION AND PARAMETER STUDY - In this section, results from a few of the test carried out with BioRID P1 are presented and compared to that of five volunteers (Table 2, Table 3).

Test set up – The BioRID P1 and volunteers were placed in a laboratory seat (Davidsson, 1999) that was mounted on a target sled (900 kg and 890 kg respectively), which was impacted by a bullet sled (530 kg and 570 kg respectively) to simulated rear impacts. The energy was transferred to the target sled by a steel bar, which was deformed during the impact (size 12*20 mm). The sled acceleration and velocity change, as derived from the 9:th degree polynomial curve-fits of the sled displacement data from the high-speed film, are shown in Figure 4 and Table 2.

Table 2. BioRID P1, test conditions for the parameter and validation study.

Thoracic spine stiffness:	Test data:	Dummy design:			Head–head restraint:
	ΔV (km/h)	Torsion pin ∅ (mm)	Rear bumper (shore 80, l*w*t mm)	Muscle subst. spring stiffness (kN/m)	Contact time (ms)
Standard	6.6	8	10*15*2	33.6	96
Increased	6.6	8	15*30'3	33.6	95
Further increased (no play between vertebrae and bumpers)	6.5	8	15*30'3	33.6	95

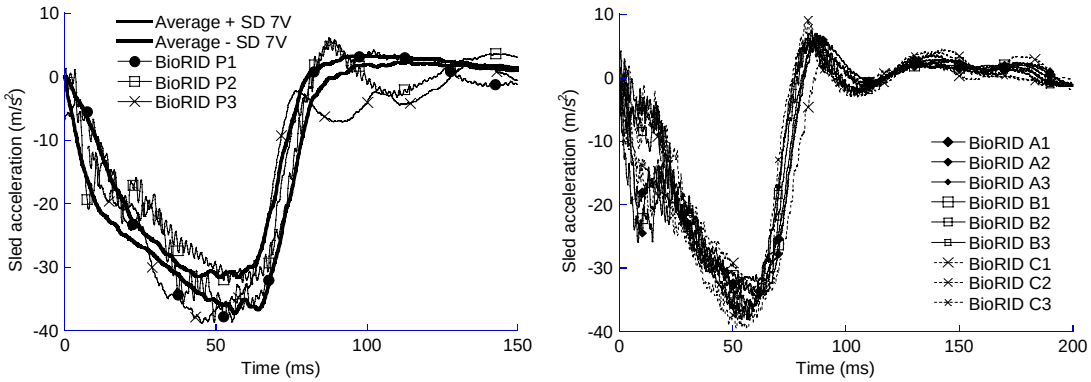

Figure 4. Typical dummy and volunteer (mean ± S.D.) sled acceleration.

Volunteers and dummy configurations - The comparison data used in this work is a sub-set, denoted 7V, of 5 tests out of a larger series of rear-end impact volunteer tests (Davidsson, 1999). The belted volunteers and dummies were seated in a normal passenger position and their arms were placed on the side of their thighs. Both volunteers and the dummy were dressed in cotton clothing. The head to head restraint distance was 102 mm for the BioRID P1 and 86 (19) mm for the average volunteer. Dummy femur and shoulder joint torque was adjusted according to chapter 3. The initial BioRID pelvis angle, defined as the angle between the horizon and the lumbar spine mounting surface (surface D in GM Hybrid III 50M drawing 78051-60) on the Hybrid III pelvis, was 26.5°. The initial H-point position was approximately constant between the tests.

Table 3. Volunteers, group 7V, test conditions.

Test:	Test data:	Anthropometry:			Head -head restraint:		
	ΔV (km/h)	Stature (m)	Weight (kg)	Age (year)	Dist. (mm)	Contact time (ms)	Pitch (°)
7V	6.7	1.81	85	35	80	80	5
	6.9	1.79	82	30	70	102	0
	6.8	1.77	65	29	120	94	0
	6.8	1.90	75	26	80	104	-5
	6.8	1.90	75	26	80	110	-8
Mean (S.D.)	6.8 (0.1)	1.83 (.06)	76 (8)	29 (4)	86 (19)	98 (12)	-2 (5)

Instrumentation - The accelerometer positions, the data acquisition, the film analysis and data processing were similar in all BioRID tests (Figure 5). Head accelerations were measured by two uniaxial accelerometers mounted inside the dummy head at a position 22 mm above and 2 mm behind of the head CG. This deviation from normal head CG accelerometer position was introduced in order to mimic the average head accelerometer position used in the volunteer study.
T1 instrumentation consisted of two uniaxial accelerometers screwed on to the T1 vertebrae. In the starting posture, the head CG and T1 x-axes were horizontal and z-axes vertical.
The seat back frame, skin of the head, T1 vertebra, skin of the upper torso and H-point were fitted with film markers (Figure 5).
Davidsson (1999) presents the volunteer instrumentation.

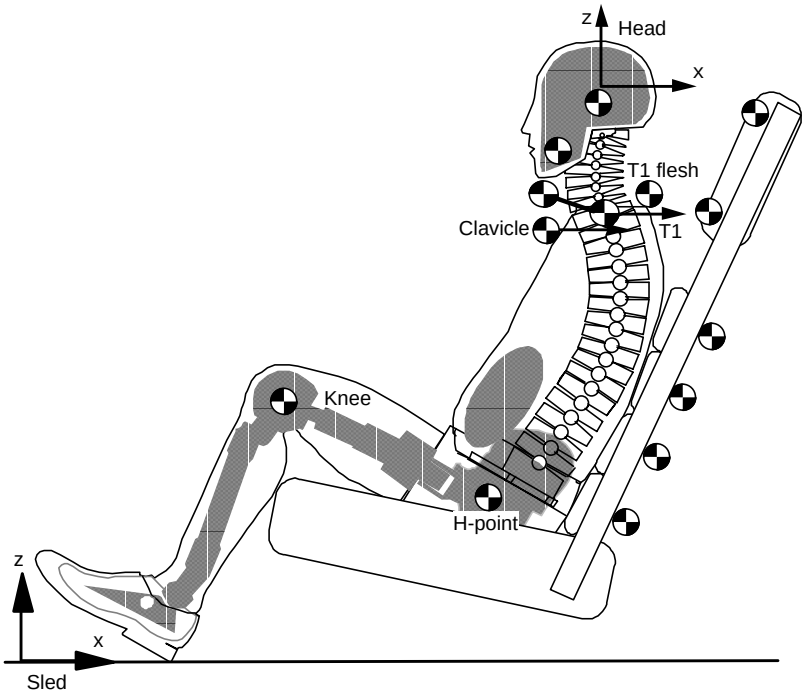

Figure 5. X-ray view of the BioRID P1 in the special seat used.

Data acquisition – Sled, head and T1 accelerometer data was sampled at 8000 Hz. All digitized data was smoothed by a mean value calculation. Window size in the mean avlue calculations were 120 for the sled x-acceleration, 20 for the head and T1 x- and z-accelerations. The tests were filmed at 500 f/s and each of the frames was digitized. Davidsson (1999) describes the data acquisition in the volunteer tests.

Coordinate systems – The BioRID anatomical coordinate systems as well as the sled fixed coordinate system are orthogonal right-handed (Figure 5). It impact start, the initial direction of the anatomical coordinate systems were parallel to the sled coordinate system. The x-axes are along the sled motion and are positive in the rearward direction. The z-axes are perpendicular to the horizontal plane and are positive in the upward direction.
Davidsson (1999) describes the coordinate systems used in the volunteer study.

Calculation of kinematics – T1 displacements are given for the center of the T1 vertebra. These displacements were estimated from two film markers mounted on the side of T1 vertebra. The upper torso angle was estimated from the clavicle marker and a film marker attached to the rubber torso posterior of T1 (Figure 5).
In order to give a single measurement of the straightening of the spine, the change of the absolute distance between T1 and H-point was calculated.
Davidsson (1999) describes the calculations of kinematics used in the volunteer study.

Results and Discussion

DUMMY DESIGN - The chosen angular range of motion (RoM) of the lumbar, thoracic and cervical spines were based on literature data.

Lumbar spine RoM - For the human lumbar spine, the average total range of motion was reported to be 15.6° (White and Panjabi, 1978) and 16.6° (Kampanji, 1974) per mobile unit. The average range of motion per mobile unit was reported to be 6° in extension and 8° in flexion (Kampanji, 1974) for a subject in standing position. To adjust for seated posture, the lumbar spine range of extension was increased and the range of flexion decreased (Andersson et al, 1979). For the BioRID lumbar spine, the range of motion was chosen to be 10° in extension and 5° in flexion.

Thoracic spine RoM - In the human thoracic spine, the total range of motion was reported to be 4-12° (average 6.3°) per mobile unit (White and Panjabi, 1978). The lowest value is for the upper and the highest value is for the lower part of the thoracic spine. For supple individuals, Kampanji (1974) attained a total range of extension of 25° and flexion of 45° for the thoracic spine in standing posture (total average range of motion of 5.8° per mobile unit). The range of motion of the BioRID thoracic spine was chosen to be 3° in extension as well as in flexion in all 12 thoracic joins. This means that the range of angular motion is somewhat higher in the BioRID compared to the average human. In a sever rear impact test with the BioRID, the chosen range of motion of the upper thorax may therefore give rice to neck and head loads lower than in a human that is subjected to a similar impact. However, data on thoracic spine RoM in seated posture is not available and future studies on thoracic spine RoM are needed.

Cervical spine RoM - For the human cervical spine, White and Panjabi (1978) reported total range of motion of 8-17° (average 12.3°) per mobile unit (8 joints) and Moffatt et al. (1979) reported 13-21° (average 16.5°) per mobile unit (8 joints). Snyder et al. (1975) reported human volunteer head relative upper torso angular displacements of 49° in extension and 55° in flexion for adult subjects in standing posture (total average range of motion of 13° per mobile unit). In the BioRID, this range was increased with 2° per unit for all 8 joints in booth flexion and extension to

allow for some hyperextension, hyper-flexion and sufficient retraction (s-shape motion)of the head.

VALIDATION AND PARAMETER STUDY – The BioRID P1 neck extension, i.e. the head relative T1 rearward angular displacement, was influenced by the thoracic spine stiffness (Figure 6). An increased thoracic spine stiffness resulted in slightly less T1 rearward displacement, which gave rice to less head-to-head restraint contact forces and, therefore, increased peak neck extension. However, peak neck extension was significant higher for increased thoracic spine stiffness and peak head angular displacement was rather similar for varying thoracic spine stiffness (Figure 6). It may be, therefore, be concluded, that the appropriate cervical stiffness, incl. the effect of the muscle substitutes, is highly depending on the thoracic spine stiffness.

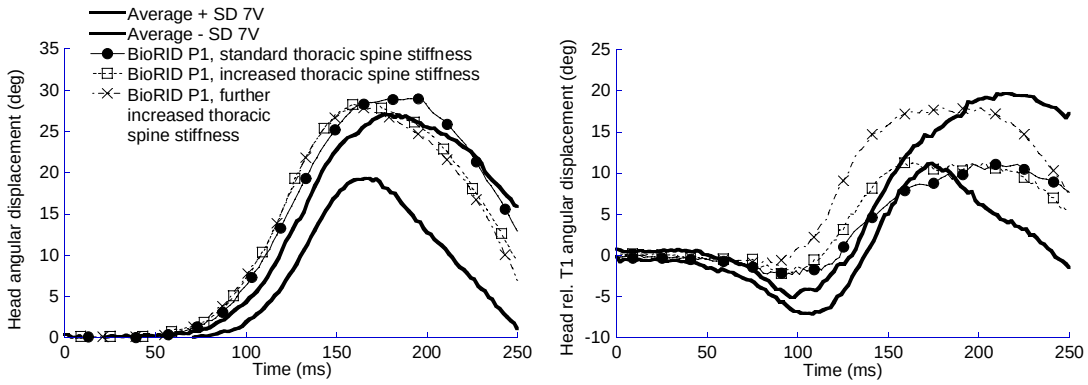

Figure 6. BioRID P1 angular displacements compared with volunteer data (mean±S.D., n=5), varying thoracic spine stiffness.

Except friction in the muscle substitutes cable systems, the BioRID P1 muscle substitutes are purely elastic. After 270 ms, the head relative T1 forward rebound angular velocity of the BioRID P1 was larger than desired (Figure 7). The data indicates that future dummy prototypes should be fitted neck muscle substitutes that incorporate a damper mounted in parallel with the elastic unit in order to reduce the angular rebound velocity between the head and T1.

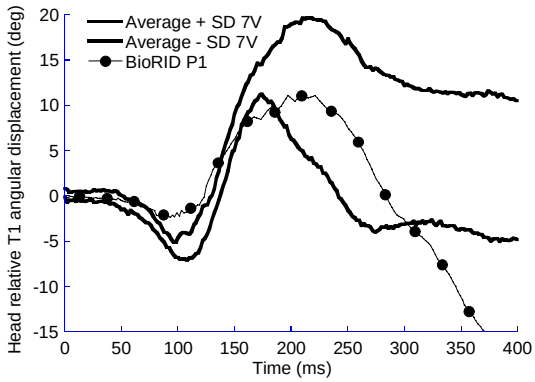

Figure 7. BioRID P1 angular displacement compared with volunteer data (mean±S.D., n=5).

For the same test, the head and head relative T1 angular displacement data (Figure 7) indicates that the neck incl. neck muscle substitutes performed biofidelic or were

slightly softer than desired with the current neck and thoracic design. The neck base did, however, not correctly load (lower neck bending moment, M_y) the T1. The peak T1 angular displacement in Figure 8 for the BioRID P1 with standard thoracic spine stiffness was too large. The data indicates that future BioRID prototypes should include stiffer thoracic spines and/or stiffer silicon torsos and/or stiffer interfaces between the torso and the upper part of the thoracic spine. In future BioRID prototypes with stiffer torsos/thoracic spines also the neck may be readjusted.

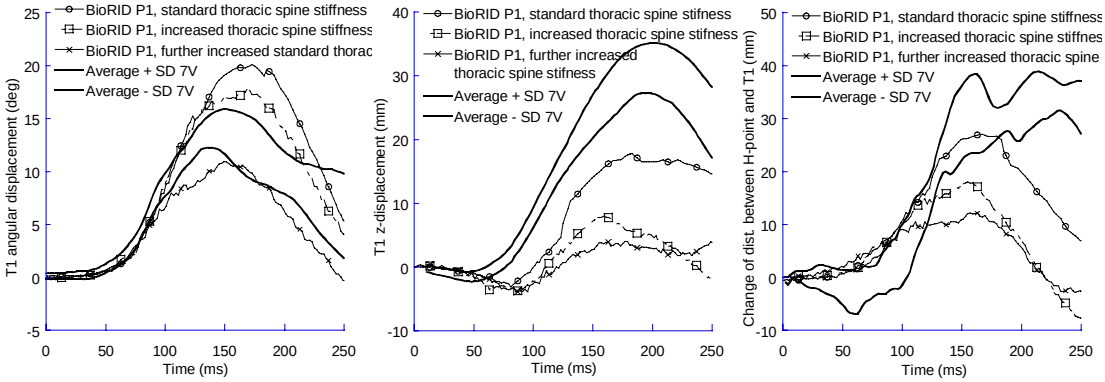

Figure 8. BioRID P1 displacements and change of distance from T1 to H-point compared with volunteer data (mean±S.D., n=5), varying thoracic spine stiffness.

In volunteer tests, McConnell et al. (1993), Davidsson et al. (1998) and Ono et al. (1997) found that during the acceleration phase of a rear-end impact, when the occupants body was pressed against the seat back, the spinal curvature straightened. This in turn caused an upward motion of the T1 and head. Tests with BioRID P1 showed that peak T1 angular displacement was too large and that the thoracic spine should be made stiffer in future BioRID prototypes. The effect of thoracic spine stiffness on T1 upward motion was evaluated in tests with BioRID P1 with varying thoracic spine stiffness. The peak T1 z-displacement was less than that of the average volunteer and was reduced as the thoracic spine stiffness was increased (Figure 8). The thoracic spine stiffness affected the straightening of the kyphosis of the thoracic spine and thereby the length of the spine, which is given in Figure 8 as the change of distance between T1 and the H-point. Future BioRID prototypes should therefore have thoracic spine stiffness similar or less than that of a standard BioRID P1 in order to mimic the human T1 z-displacements.

Conclusions

- The thoracic spine stiffness highly influences the motion of the neck.
- Except for elastic units, the neck muscle substitutes should also include damping units in order to decrease rebound velocity of the head relative T1.
- Thoracic spine stiffness should be increased in order to decrease peak T1 rearward rotation.
- Torso stiffness and its interface to the thoracic spine should be increased in order to decrease T1 rearward rotation.
- Thoracic spine stiffness should not be increased in order not to reduce the T1 upward displacement.

1.4 BioRID P2 and BioRID I

Materials and methods

DUMMY DESIGN - The second BioRID prototype was quite different from its predecessor, the BioRID I. The following parts were either different in design or were made in materials with different properties from that of the predecessor:

- The thoracic torsion pin diameter was 10 mm (8 mm for the BioRID P1) while the lumbar spine torsion pin diameter was the same as that of the BioRID P1, i.e. 8 mm.
- The vertebrae were made in durable plastic (aluminum for the BioRID P1).
- The cervical vertebrae were redesigned with an improved geometry and with increased durability while the thoracic and lumbar vertebrae were similar to those of the BioRID P1.
- Torso was made in Wacker M4601 A+B silicon that was mixed with silicon oil. The material was slightly softer than that of the BioRID P1.
- A water filled cavity was fitted the abdomen in order to reduce torso resistance to flexion/extension (no water filled cavity in BioRID P1).
- The upper part of the rubber torso was cut at two levels in order to reduce torso stiffness (the BioRID P1 torso was cut at four levels).
- The total number of spine-torso interface pins were 15 (the BioRID P1 was fitted with a total of 30).
- The neck muscle substitutes were connected to a damper in parallel to a spring. The damping constant was approximately 2.6 kNs/m and the spring constant was 12.1 kN/m (for the BioRID P1 the spring constant was 33.6 kN/m, no damper).
- The dummy was dressed in 2 layers of shirt and pants made of Lycra knitted fabric (BioRID P1 was dressed in cotton clothing).
- The dummy was fitted a modified Hybrid III seated pelvis (BioRID P1 was fitted a Hybrid III pedestrian pelvis).

The BioRID I design is similar to that of the BioRID P2 (see Table 4). The torso did not have any horizontal cuts (Figure 9). The BioRID I muscle substitutes had slightly stiffer cable/cables houses than in the BioRID P2. The spring-damper unit had a spring stiffness that was 16.8 kN/m and a damping constant that was approximately 8 kNs/m. In the inter-spaces between the thoracic vertebrae, there were placed rubber elements. In the BioRID I these blocks were thicker and softer than in the BioRID P2, 3 mm of shore 40 polyurethane and 2 mm of shore 80 polyurethane respectively, in order to increase the progressiveness of the flexion/extension resistance. The other dimensions and the position of these rubber blocks were unchanged.

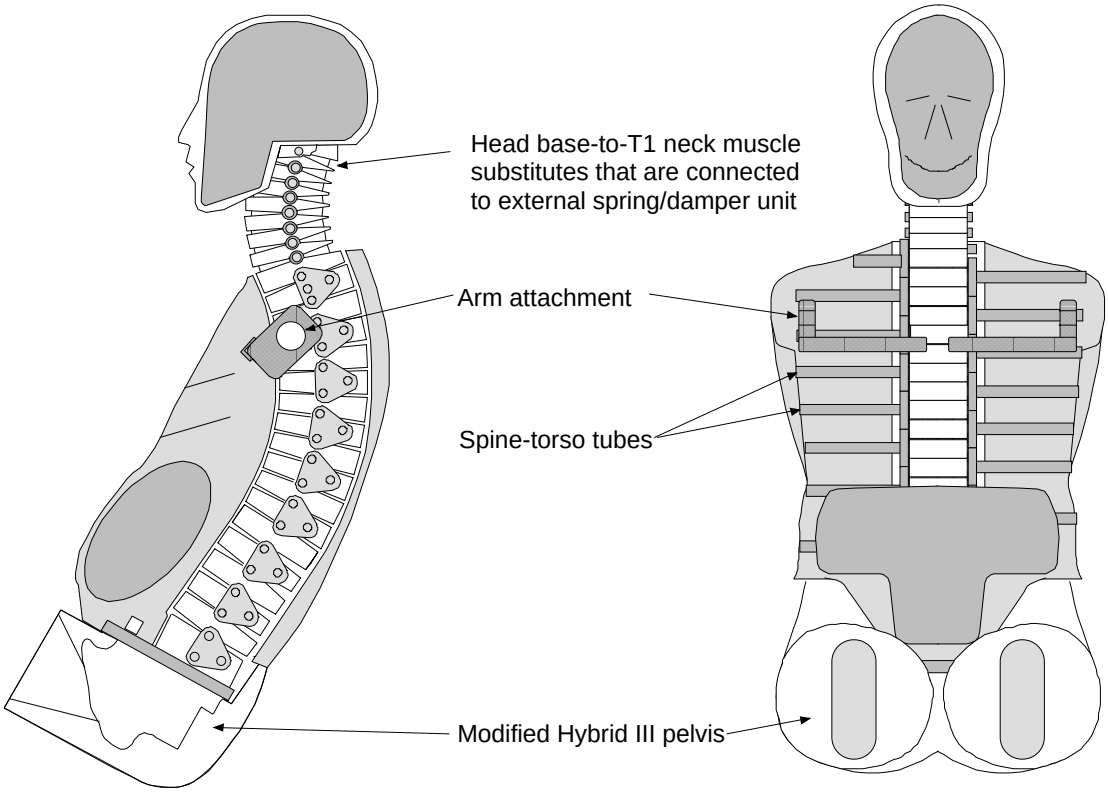

Figure 9. X-ray view of parts of the BioRID P2.

PARAMETER AND VALIDATION STUDY - In this section, results from a few of the test carried out with BioRID P2 are presented (Table 4, Table 5 and Table 6).

The BioRID P2 tests were carried out in the same seat and sled, with the same instrumentation, data acquisition, coordinate systems and calculation of kinematics as in the BioRID P1 tests. Also the same evaluation data, similar dummy adjustments, similar initial posture were used in the BioRID P2 study as those used in the BioRID P1 study

The BioRID P2 sled velocity change was 6.6 km/h and the sled acceleration is shown in Figure 4. For the parameter tests with BioRID P2, the sled velocity changes, the derivative of the 9:th degree polynomial curve-fits on the sled displacement data from the high-speed film, are presented in Table 4, Table 5 and Table 6.

Table 4. BioRID P2, test conditions, neck muscle substitute characteristics.

Test:	Test data:	Muscle substitute characteristics:			Head –head restraint:
	ΔV (km/h)	Damping (kNs/m)	Stiffness spring (kN/m)	Stiffness cable /cable house	Dist. x –dir. (mm)
Lower spring stiffness than standard	6.6	2.6 (Std.)	0	Standard	110
Standard spring stiffness	6.5	2.6	12.1 (Std.)	Standard	110
Standard cable/cable house	6.3	8.0	16.8	Standard	90
Higher cable/cable house stiffness than standard	6.3	8.0	16.8	High	90
Higher damping characteristics than standard	6.3	8.0	16.8	High	90
Standard damping characteristics	6.2	2.6	16.8	High	90
None pre-tensed posterior muscle substitute	6.3	2.6	16.8	High	90
Pre-tensed posterior muscle substitute	6.3	2.6	16.8	High	90

Std standard

Table 5. BioRID P2, test conditions, friction between dummy and seat.

Test:	Test data:	Clothing:	Muscle substitute characteristics:			Head –head restraint:
	ΔV (km/h)		Damping (kNs/m)	Stiffness spring (kN/m)	Stiffness cable /cable house	Dist. x –dir. (mm)
Higher friction than standard, n=3	6.5 (0.09)	Lycra	2.6	12.1	Standard	110
Standard friction, n=3	6.6 (0.05)	2x Lycra	2.6	12.1	Standard	110

Table 6. BioRID P2, test conditions, thoracic spine design.

Test:	Test data:	Dummy design:	Muscle substitute characteristics:			Head –head restraint:
	ΔV (km/h)	Rear thoracic spine bumper	Damping (kNs/m)	Stiffness spring (kN/m)	Stiffness cable /cable house	Dist. x –dir. (mm)
Standard rubber elements	6.3	15*10*2 Shore 80	8.0	16.8	Standard	90
No rubber elements	6.2	None	8.0	16.8	Standard	90

REPEATABILITY AND REPRODUCIBILITY STUDY - Three BioRID I:s (A, B and C) were tested three times each under identical conditions, which were similar to those used in the validation tests (Table 3). In these test, the same head, pelvis, upper and lower extremities were fitted the different BioRIDs. The seat and sled test setup was the same in the repeatability tests as in the parameter tests. The BioRID I:s were dressed in two layers of Lycra clothing. The head to head restraint distances were 90 mm, the H-points were carefully adjusted until their locations were the same in all tests. Sled accelerations are shown in Figure 4. Sled velocity changes for three repeated tests with three BioRID I (A, B and C) were 6.14 (0.07), 6.17 (0.09) and 6.26 (0.20) km/h respectively. An analysis of variance was used to calculate separate coefficients of variation (C.V.) for repeatability and reproducibility. The $C.V._{\cdot\text{Repeatability}}$ and $C.V._{\cdot\text{Reproducibility}}$, which are measures of variability expressed as a percentage of the mean peak value, are defined below.

$$C.V._{\cdot\text{Repeatability}} = \left[\frac{s_p}{\overline{\overline{X}}_g}\right] * 100\%$$

$$C.V._{\cdot\text{Reproducibility}} = \left[\frac{\tau}{\overline{\overline{X}}_g}\right] * 100\%$$

Where:

$$s_p^2 = \sum_{t=1}^{k}\sum_{i=1}^{n_t}\frac{(y_{ti} - \bar{y}_t)^2}{N-k}$$

$$\tau^2 = s_g^2 - \frac{s_p^2}{k}$$

$$s_g^2 = \sum_{t=1}^{k}\frac{(\bar{y}_t - \bar{y})^2}{k-1}$$

$\overline{\overline{X}}_g$ = grand mean of all nine BioRID I tests

s_p = estimated pooled standard deviation of all three BioRID I

t = t : th test series

i = i : th test in the t : th test series

N = total number of tests

τ = standard deviation between the three BioRID I

s_g = standard deviation between averege of all tests in t : th test series and all tests

Results and Discussion

DUMMY DESIGN – The bonding between the BioRID P2 torso rubber and its arm attachments turned loose. In future BioRID prototypes, the arm attachments should be made in aluminum (instead of steel) in order to increase the strength of the chemical bonding and made larger in order to increase the bonding surface.

A stronger neck muscle substitutes cable should be chosen for future BioRID prototypes in order to increase the durability.

The top cervical vertebra to the head attachment turned loose during testing and should bee redesigned in future BioRID prototypes in order to increase its repeatability and durability.

VALIDATION STUDY - The BioRID P2 thoracic spine stiffness was tuned in order to give T1 angular and x-displacements that resembled those of the volunteers. Tests with BioRID P1showed that the thoracic spine influenced the T1 z-displacement. It was concluded that a stiffer thoracic spine resulted in reduced straightening of the kyphosis and thereby reduced upward motion of T1. The BioRID P2 T1 z-displacements are too small, the change of distance between T1 and the H-point (elongation of the thoracic and lumbar spine) are too small and the H-point z-displacement is similar to those of the average volunteer. Future BioRID prototypes should, in order to resemble the human's T1 upward motion, incorporate thoracic spines with less stiffness than that of BioRID P2.

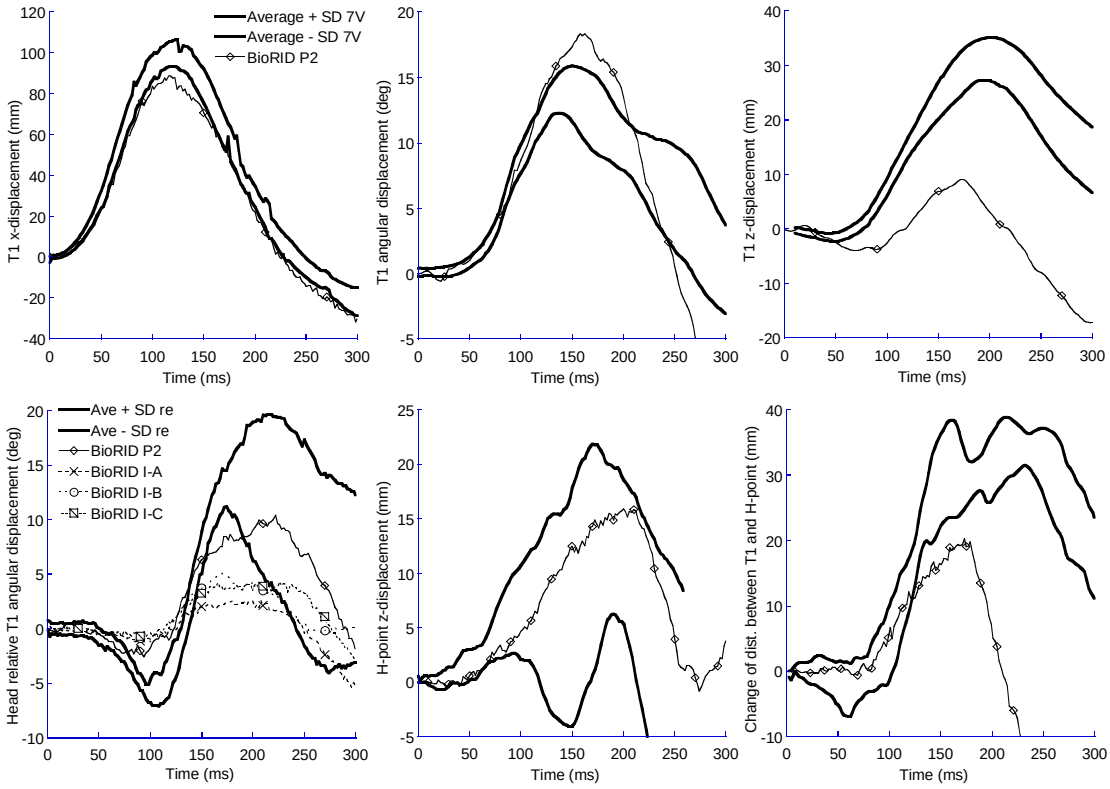

Figure 10. BioRID P2 displacements compared with volunteer corridors (mean±S.D., n=5).

Unfortunately, a reduction of the thoracic spine stiffness would also give rise to a larger T1 angular displacement than desired. In the BioRID P2, the spine-torso pins mainly prevent linear displacement between the spine and torso (Figure 11). In the future BioRID prototypes, a new interface, which would also reduce angular displacement between the T1 and torso, should be introduced. This interface would increase the resistance to T1 angular displacement with maintained resistance to T1 x-displacement.

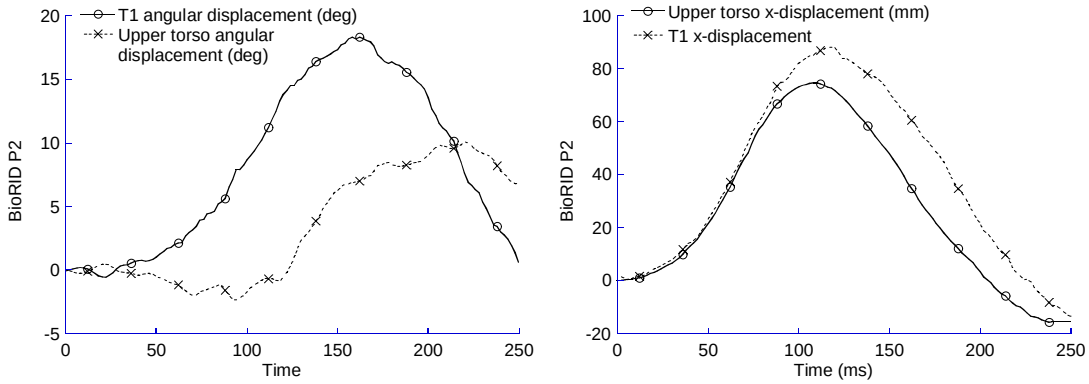

Figure 11. BioRID P2, upper torso and T1 displacements.

A reduction of the thoracic spine stiffness is desirable since it would result in larger T1 z-displacements and elongation of spine length. In the BioRID P2, the muscle substitute loads are transferred to the T1 vertebra only. If the thoracic spine stiffness was to be reduced, the neck loads would give rice to excessive T1 rearward rotation. However, if the neck muscle substitute loads were to be distributed on a number of the upper thoracic vertebrae, the T1 angular displacement would most likely become closer to that of the average volunteer.

PARAMETER STUDY – The effect of changes introduced to the neck muscle substitute system was evaluated on a BioRID P2. The characteristics of the springs and damper that were connected to the muscle substitutes in the BioRID P2 were varied (Table 4) and the effect on head relative T1 angular displacement was studied (Figure 12). Only a very small effect was observed when the damping constant or the spring stiffness was changed. These changes were difficult to distinguish from the "noise" caused by variations e.g. in initial seating posture. The head relative T1 angular displacement changed, however, considerably when the cable house stiffness was increased (Figure 12). In the BioRID P2, the neck muscle substitute loads were transferred from T1 vertebra to the damper/spring unit. This unit had, due to the size of the damper, to be placed on the outside of the dummy and, consequently, the cable/cable house had to be rather long. The stiffness of the chosen cable house was too low. Effects on head relative T1 angular displacement on the changes introduced to the damper/spring unit was probably compensated for by elastic changes in the cable /cable house length (Figure 12). Future BioRID prototypes should be fitted with softer damper/spring and the damper/spring unit should be fitted as close to the T1 as possible, to reduce the length and thereby the elastic effect of the cable/cable house.

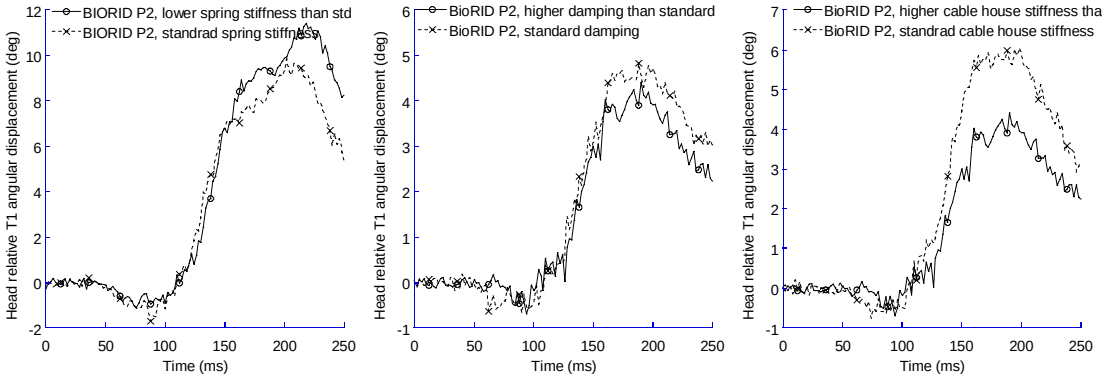

Figure 12. BioRID P2, various spring stiffness, head relative T1 angular displacement.

In many parameter studies, it is important to maintain a constant head to head restraint distance. The effect of forcing the head forward, in order to increase the head to head restraint distance prior to test, was evaluated in this parameter study (Table 4). The anterior neck muscle substitute was lengthened and the posterior neck muscle substitute was shortened until the neck was extended approximately 10 deg. The dummy neck was thus slightly extended in comparison to normal sitting posture. Prior to the test the head was positioned at standard distance from the head restraint and the neck curvature was then returned to normal. A BioRID with the neck muscle substitutes unchanged was tested for comparison. At impact, the peak head relative T1 angular displacement was much larger for the modified dummy than for the standard dummy (Figure 13). To conclude, it is vital that proper head to head restraint distance is achieved by adjusting the neck cable lengths and/or the thoracic and lumbar spine curvature. The head must not be forced rearward or forward in order to achieve desirable head to head restraint distance prior to test.

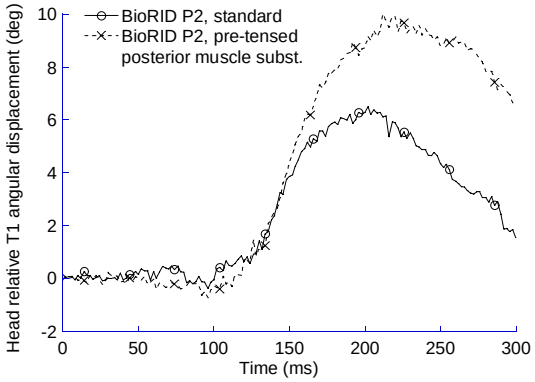

Figure 13. BioRID P2, pre-tensed posterior and standard muscle substitutes.

As previously concluded, the thoracic spine stiffness should be reduced in future prototypes relative that of the BioRID P2 in order to increase the T1 upward motion. Both the torsion bars and the rubber blocks placed between adjacent vertebra control the thoracic spine stiffness. In order to investigate the effect of redesigning the rubber elements for the next BioRID prototype, the posterior rubber elements of a BioRID P2 thoracic spine (T3-T4 to T12-L1 posterior rubber elements removed) were removed (Table 6) and the T1 angular displacement was compared to that of a standard BioRID

P2 (Figure 14). The data indicates that the rubber elements did not influence the T1 angular displacement. Consequently, the diameter of the thoracic spine torsion bars should be made thinner in future BioRID prototypes in order to increase the T1 upward motion.

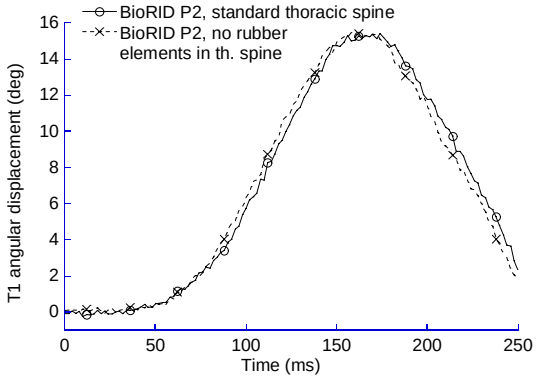

Figure 14. BioRID P2, effect on T1 angular displacement of posterior rubber blocks in the thoracic spine.

In a comparison between human volunteer kinematics and the first version of BioRID P2, it was concluded that the dummy H-point and T1 z-displacements were smaller than those for the volunteers. The effect of friction between dummy and seatback/cushion on T1 z-displacement was evaluated in a parameter study (Table 5). Repeated tests with a BioRID P2 dressed in either a single or double layer Lycra clothing was performed. The H-point and T1 z-displacements were larger for the dummy dressed in two layers of Lycra than for the dummy dresses in a single layer of Lycra (Figure 15). The results indicate that the BioRID P2 should be dressed in two layers of Lycra.

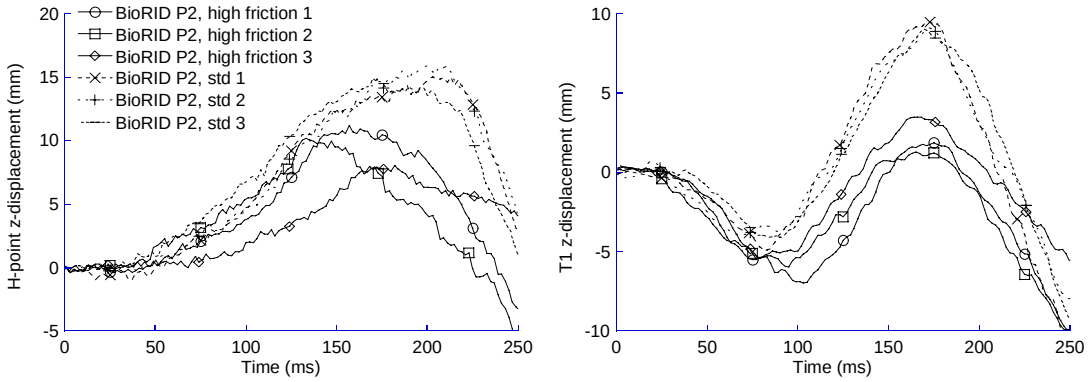

Figure 15. BioRID P2, the effect of friction between dummy and seat surfaces on dummy kinematics (high friction = single layer Lycra, standard friction = double layer friction).

REPEATABILITY AND REPRODUCIBILITY STUDY – Repeatability and reproducibility are major considerations in the evaluation of test dummy design. Low overall accuracy in car seat evaluation tests are due to poor dummy repeatability and reproducibility in combination with small sample size. According to Wismans et al. (1994) a C.V. of 5% or less is considered to be good and a C.V. of 10% or less is

considered acceptable. The BioRID Is' C.V. was below 5% for all parameters included in
Table 7, which indicate that the dummy repeatability was good for the parameters studied.

The data also indicate that the BioRID I design is reproducible, which as indicated by all parameters except upper neck Fx.

Table 7. Coefficient of variation for the BioRID I.

Parameter:	Repeatability BioRID I (CV%)	Reproducibility BioRID I (CV%)
Head x-displacement (%)	1	2
T1 x-displacement (%)	2	0
Head angular displacement (%)	5	0
T1 angular displacement (%)	5	0
T1 x-acceleration (%)	3	1
T1 z-acceleration (%)	5	1
Upper neck My	5	0
Upper neck Fx	8	16
Upper neck Fz	5	3

Conclusions

- The cable and cable houses that transferred the neck loads between T1 and the damper/spring unit should be shortened, made stiffer and the friction between the cable and the cable house should be as low as possible.
- Future BioRID prototypes should most likely be fitted anterior neck muscle substitutes that have a damping constant and spring stiffness lower than that of BioRID P2 and BioRID I in order to better mimic the human volunteer head relative T1 rearward angular displacement.
- Thoracic spine stiffness should be decreased in order to increase the T1 upward motion.
- The arm attachments should be made stronger and neck muscle substitute cables thicker in order to increase durability.
- The BioRID should be dressed in two layers of Lycra clothing in order to facilitate biofidelic ramping up along the seat back.
- A stiffer interface between the upper part of the thoracic spine and the rubber torso should be introduced in future BioRID prototypes in order to reduce the T1 rearward angular displacement.
- The BioRID I was repeatable and the dummy design was reproducible.

1.5 BioRID P3 and BioRID II

Materials and methods

DUMMY DESIGN - The third BioRID prototype was further refined in a number of ways. The following parts were either different in design or was made in materials with different properties from that of the predecessor, the BioRID P2:

- The thoracic and lumbar spine torsion pin diameter was 8 mm (BioRID P2 thoracic spine torsion pin diameter was 10 mm).
- The torso was made in a softer silicon than in BioRID P2 (Wacker RT 623 A+B silicon that was mixed with silicon oil).
- There were no cuts in the upper part of the silicon torso (BioRID P2 was cut at two levels).
- A stiffer torso-spine interface was introduced in the BioRID P3.
- The BioRID P3 was fitted with 2 pairs of neck muscle substitutes that equally distributed the neck loads on T1, T2 and T3.
- The left and right neck muscle substitute pairs were connected to a rotational damper and coil springs, respectively. The damping constant was approximately 310 Ns/m. The anterior and posterior muscle substitute spring constants were 12.1 kN/m and 9.8 kN/m respectively. The springs and damper was fitted inside the torso.
- The arm attachments were redesigned in BioRID P3. This was done in order to increase the shoulder motions and increase the strength of the shoulder to torso joint.
- The abdomen to pelvis attachment was made larger in order to increase the durability of the dummy.
- The dummy was dressed in two layers of shirt and pants made of Lycra.

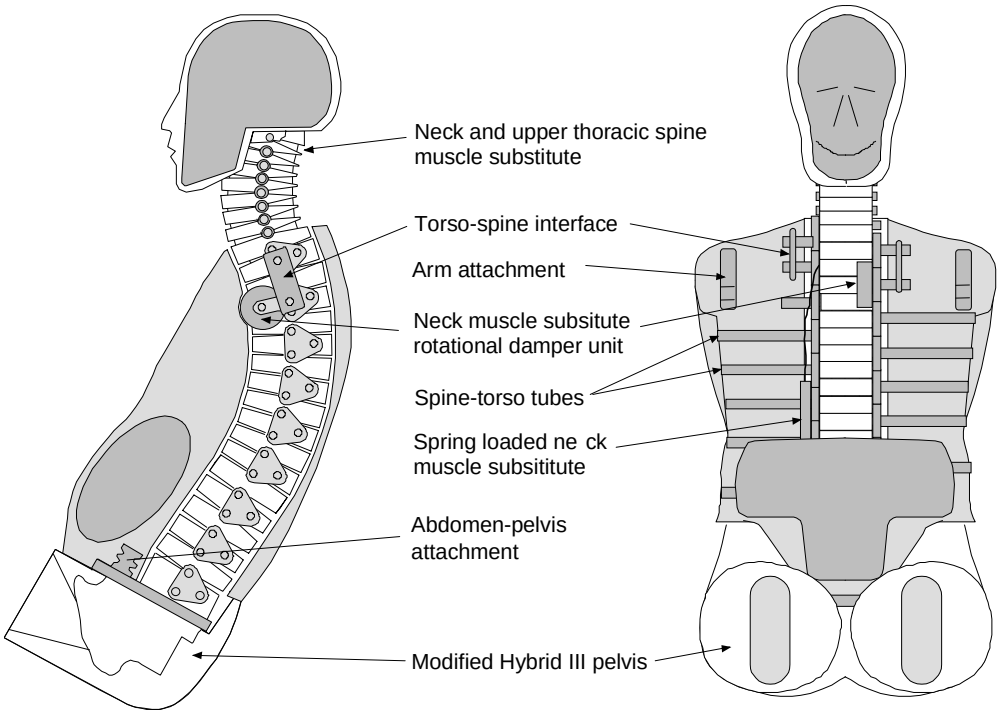

Figure 16. Schematic of parts of the BioRID P3.

VALIDATION STUDY – The BioRID P3 was compared to volunteer kinematics in two companion papers (Davidsson et al. 1999a and 1999b). In this report a few of the findings in those articles will be highlighted.

Results and Discussion

DUMMY DESIGN – The BioRID P3 torso-spine interface bonding surface was too small. In future prototypes the surface of the torso-spine interface should be larger in order to increase the durability of the dummy and to reduce peak T1 rearward angular displacements.

The BioRID P3 abdomen-pelvis attachment was too small and should be made larger in future dummy prototypes in order to increase durability.

The BioRID II design is similar to that of the BioRID P3 (Davidsson et al. 1999b). The BioRID II was fitted larger torso-spine interfaces, larger abdomen-pelvis attachment, and a smaller abdomen cavity (in order to fit a larger abdomen-pelvis attachment) and minor modifications introduced to the design of the rotational damper. These design changes were introduced in order to make the dummy more user-friendly or/and to increase the durability of the dummy. The changes will most likely not affect the kinematic performance of the dummy.

VALIDATION STUDY – The BioRID P3 neck resistance to extension was found to be close to that of the human in a rigid and standard seat without head restraint (Davidsson et al. 1999a) and in a laboratory seat (Davidsson et al. 1999b). In the latter study it was concluded that the BioRID P3 neck s-shape (retraction motion) was larger than that of the humans. In the former study, the resistance to neck s-shape motion was only slightly less for the BioRID P3 than for the human volunteers. In future BioRID prototypes test with increased resistance to neck s-shape motion, i.e. the inter-vertebral resistance to extension/flexion, should be performed and the results evaluated.

In Davidsson et al. (1999a) it was shown that the initial as well as the peak pressure distributions between the BioRID P3 and the seat back was different from those of a representative volunteer in the standard seat. At maximum pressure, the seat loaded the volunteer's lumbar spine erector muscles, thoracic vertebra processes and medial part of the scapula bones. In the BioRID P3 test, the seatback loaded the distal part of the dummy torso and the pelvis back.
In future BioRID prototypes, the following three design changes should be considered:

- The dummy rubber torso material should be softer.
- The dummy back surface geometry should be changed. Especially the lateral parts of the back surface.
- The overall dummy torso stiffness should be decreased.

The BioRID P3 rebound head and T1 forward linear and angular velocity were too large (Davidsson et al. 1999a). Future prototypes should preferably include energy absorbing units mounted in parallel with rear thoracic and cervical rubber bumpers.

The future prototypes should also preferably be fitted torsos that can absorb energy to a larger extent than the silicon torso did.

The iliac crest and the H-point horizontal peak displacements were larger for the volunteers than for the BioRID P3 (Davidsson et al. 1999a and 1999b). The data indicate that the BioRID P3 pelvis rear surface compliance was different from that of the human volunteers. Future BioRID prototypes should preferably be fitted a pelvis with softer pelvis flesh.

REPEATABILITY STUDY – The results from a repeatability study performed with the BioRID P3 is presented by Davidsson et al. (1999b). The coefficient of variation was 5% or less for all reported parameters and the dummy repeatability was therefore considered good.

Conclusions

The torso-spine interface and abdomen-pelvis attachment should be made larger in order to increase the torso durability in future BioRID prototypes.

The rubber torso rubber material stiffness, torso back surface geometry and overall dummy rubber torso stiffness, or a combination of these, should be reduced/changed in future BioRID prototypes in order to increase the biofidelity of the seat back to dummy back interactions.

1.6 References

Andersson, G.B.J., Murphy R.W., Örtengren, R., Nachemson (1979) The Influence of Backrest Inclination and Lumbar Support on Lumbar Lordosis. Spine, Vol. 4, No. 1, pp. 52-58.

Davidsson, J., Deutscher, Hell, W., Linder, A., Lövsund, P., Svensson, M.Y. (1998) Human Volunteer Motion in Rear-End Sled Collisions. Proc. 1998 Int. IRCOBI Conf. pp. 289-301.

Davidsson J. (1999) Human Volunteer Kinematics in Rear-End Sled Collisions. Report November 1999, Crash Safety Division, Department of Machine and Vehicle Design, Chalmers University of Technology, Göteborg.

Davidsson, J., Lövsund, P., Ono, K., Svensson, M.Y., Inami, S. (1999c) A Comparison between Volunteer, BioRID P3 and Hybrid III performance in Rear Impacts. Proc. 1999 Int. IRCOBI Conf., pp. 165-178.

Davidsson, J., Flogård, A., Lövsund, P., Svensson, M. Y. (1999b) BioRID P3 - Design and Performance Compared to Hybrid III and Volunteers in Rear Impacts at ΔV=7 km/h. 43rd Stapp Car Crash Conf., SAE 99SC16, pp. 253-265.

Dvorak, J., Froehlich, D., Penning, L., Baumgartner, H., Panjabi, M. M. (1988) Functional Radiographic Diagnosis of the Cervical Spine: Flexion/Extension, Spine, Vol. 13, No. 7, pp. 748-755.

Dvorak, J., Panjabi, M. M., Chang, D. G., Theiler, R., Grob, D. (1991) Functional Radiographic Diagnosis of the Lumbar Spine, Spine, Vol. 16, No. 5, pp. 562-571.

Deng, Y.-C. (1989) Anthropomorphic Dummy Neck Modelling and Injury Considerations. Accid. Anal. & Prev. Vol. 21, No 1, pp. 85-100.

Foret-Bruno, J.Y., Dauvilliers, F., Tarriere, C., P. Mack (1991) Influence of the Seat and Head Rest Stiffness on the Risk of Cervical Injuries in Rear Impact. Proc. 13th Int. Conf. on Enhanced Safety of Vehicles, paper 91-S8-W-19.

McConnell, W. E., Howard, R. P., Guzman, H. M., Bomar, J. B., Raddin, J H., Benedict, J. V., Smith, L. H., Hatsell, C. P. (1993) Analysis of Human Test Subject Responses to Low Velocity Rear End Impacts. SAE 930889, -975, pp. 21-30.

Moffatt, E.A., Schulz, A.M. (1979) X-ray study of the Human Neck during Voluntary Motion. SAE 790134, P-79/438, pp. 31-36.

Ono, K., Kaneoka, K., Wittek, A, Kajzer, J. (1997) Cervical Injury Mechanism based on the Analysis of Human Cervical Vertebral Motion and Head-Neck-Torso Kinematics during Low Speed Rear Impacts. SAE, LC 67-22372, pp. 339-356.

Robbins, D. H. (1985) Antropometry of Motor Vehicle Occupants. Vol. 2 (3), U. S. Department of Transportation, NHTSA, DOT HS 806 716.

Seemann, M.R., Muzzy, W.H., Lustick, L.S. (1986) Comparison of Human and Hybrid III Head and Neck Response. Proc. 30th Stapp Car Crash Conf., SAE 861892, pp. 291-312.

Snyder, R. G., Chaffin, D. B., Foust, D. R. (1975) Bioengineering study of basic Physical Measurements related to Susceptibility to Cervical Hyperextension-Hyperflexion Injury. University of Michigan, Highway Safety Research Inst., UM-HSRI-B1-75-6.

Svensson, M. Y. and Lövsund, P. (1992) A Dummy for Rear-End Collisions - Development and Validation of a New Dummy-Neck. Proc. 1992 Int. IRCOBI Conf., pp. 299-310.

Tarriere, C. and Sapin, C. (1969) Biokinetic Study of the Head to Thorax Linkage. Proc. 13th Stapp Car Crash Conf., pp. 365-380.

Thunnissen, J.G.M., Ratingen, M.R. van, Beusenberg, M.C., Janssen, E.G. (1996) A Dummy Neck for Low Severity Impacts. Proc. Int. Conf. on Enhanced Safety of Vehicles, 96-S10-O-12.

Tisserand, M. and Wisner, A. (1966) Comportement du Rachis Cervical lors de Chocs Dorsaux. Center de Physiologie du Travail de l'Institut National de Securite, Report no. 73.

White III, A. A. and Panjabi, M. M., (1978) Clinical Biomechanics of the Spine. J. B. Lippincott Company, Philadelphia, USA, ISBN 0-397-50388-1.

Wismans, J., Janssen, E.G., Beusenberg, M., Koppens, W.P., Lupker, H.A. (1994) Injury Biomechanics. Third term W-3.3, WMT-3.3, Code 4J610, TNO Crash-Safety Research Center, Box 6033, 2600 JA Delft, The Netherlands.

2 Handling and storage of BioRID II

This chapter describes how to correctly handle the BioRID. The BioRID is a delicate measurement device and should be handled with care. Please, follow the recommendations below in order not to damage the dummy.

2.1 Lifting the BioRID

The BioRID may not be lifted in the head or arms. The dummy should preferably be lifted by the pelvis flag attachment and spine-torso interface (Figure 17). The stresses induced on the dummy will then not change its performance.

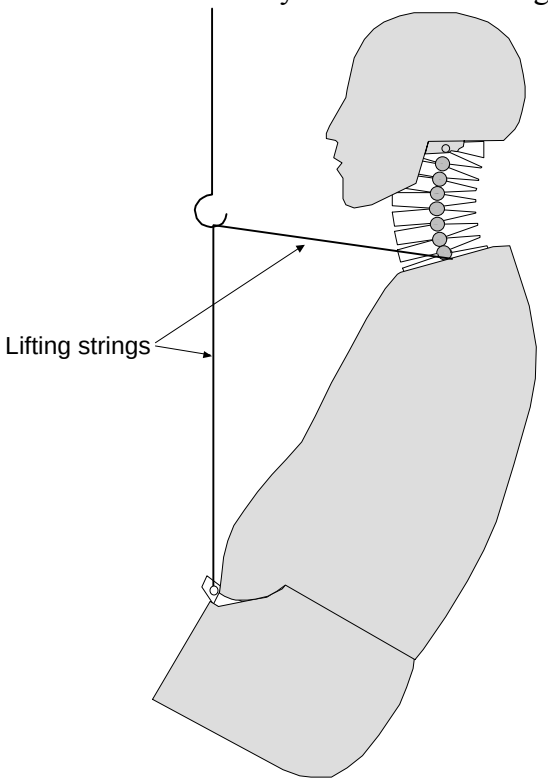

Figure 17. Illustration of lifting procedure

2.2 Handling the torso

The torso of the BioRID is a moulded silicon structure with a canal for the spine (Figure 18). The torso is connected to the spine by means of spine-torso pins. In the upper part of the torso, these pins load the spine-torso interface (Figure 18). The shoulder yokes are attached to the arm attachments and the lower part of the torso is attached to the pelvis interface by means of an abdomen attachment. These attachments and interfaces are moulded into the torso. In the lower part of the torso, there is a cavity filled with water (volume 2060 ml, BioRID II only) simulating the human abdomen.

When handling the dummy torso, follow the recommendations below:

- Do not cut parts away from the torso. The moulded silicon torso is a load bearing part of the dummy.

- Tears and fissures should be mended immediately since the material has low tearing resistance. However, it is possible to attach markers to the silicon torso, using fine steel wire.
- The silicon material may be repaired with Wacker M4601 A+B silicon. Aluminum parts that are to be moulded into the dummy torso should preferably be primed with Wacker G790 primer before moulding/repair.
- Please, check on regular bases that the abdomen attachment, arm attachments and the torso-spine interface are not loose. The quality of the bonding between the interfaces/attachments and the silicon rubber effects the dummy response.
- Sharp objects should be kept away from the dummy's torso. The silicon around the abdomen cavity is rather thin and vulnerable.
- Do not move the dummy or position the dummy by pulling in the arms. Due to the design of the arm attachments, there is a risk of damage if this is done.
- The silicon rubber in combination with the Lycra clothes worn by the dummy can produce static electricity. It is advisable to ground the dummy’s head and metal parts of the spine and pelvis. There are M8 screw holes in the lower part of the spine available for grounding purposes.

2.3 Handling the spine

The spine is made of durable plastic vertebrae, aluminum interfaces, steel pin joints, steel washers, polyurethane rubber bumpers, steel cables and springs. Handling is not likely to damage the design or change the material properties. It is, however, recommended that the BioRID II be stored with its head dismounted and the front neck muscle substitutes released approximately 10 mm. The dummy should be stored with the spine in a normal curvature in order to avoid excessive load on the rubber blocks in between the vertebrae, see section 4.1.

3 Assembly of BioRID II

This chapter describes the parts of the BioRID II (Figure 18) and how they should be assembled. Each section starts with a short description of the inherent parts and is followed by assembly instructions.

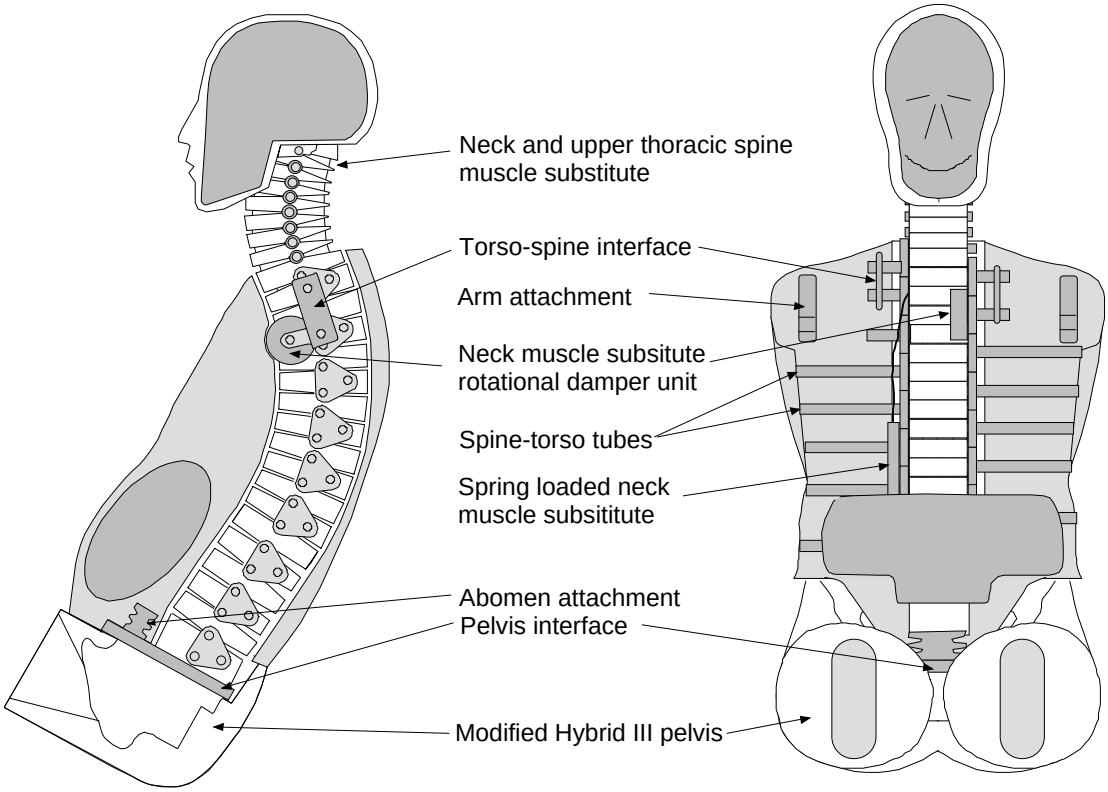

Figure 18. X-ray view of the BioRID II dummy (excluding arms, shoulders and legs).

3.1 Spine

Inherent parts - Below is a list of all parts of the spine:
Pelvis interface (Figure 19).
Occipital interface (Figure 20).
S1 vertebra with rubber bumpers (Figure 19).
Lumbar vertebrae with rubber bumpers (L1-L5, Figure 21).
Thoracic vertebrae with rubber bumpers (T1-T12, Figure 21).
Cervical vertebrae with rubber bumpers and bottoming out stops (C1-C7, Figure 21).
Torsion pins (17 pieces, Figure 22).
Torsion thoracic washers (10 pieces, cc=26,5 mm, Figure 22).
Torsion lumbar washers (6 pieces, cc=30,5 mm, Figure 22).
Torsion T4 washer (Figure 22).
T4 washer to T4 vertebra shim washer (total thickness of 1.6 mm).
Torsion T1 washer (Figure 22).
Torsion adjustment washers (17 pieces, Figure 22).
Adjustment screws (17 pieces, K6S, M8x10, grade 6 (12.9), Figure 22).
Pelvis interface-S1 attachment screws (4 pieces, MF6S, M6x20).
Cable guide wheel (1 piece).
S1-shim washer (total thickness of 1.6 mm).

H-point position indicator attachment screw (2 pieces M8*30).
Neck joint pins (5 pieces, steel, Ø8 mm, length 60 mm).
T1-C7 joint pin and nuts (threaded 20 mm at each end, steel Ø8 mm and 4 M8 nuts).
C1-C2 joint pin (1 piece, length 78 mm).
Head-occipital-C1 joint pin (1 piece, length 100 mm).

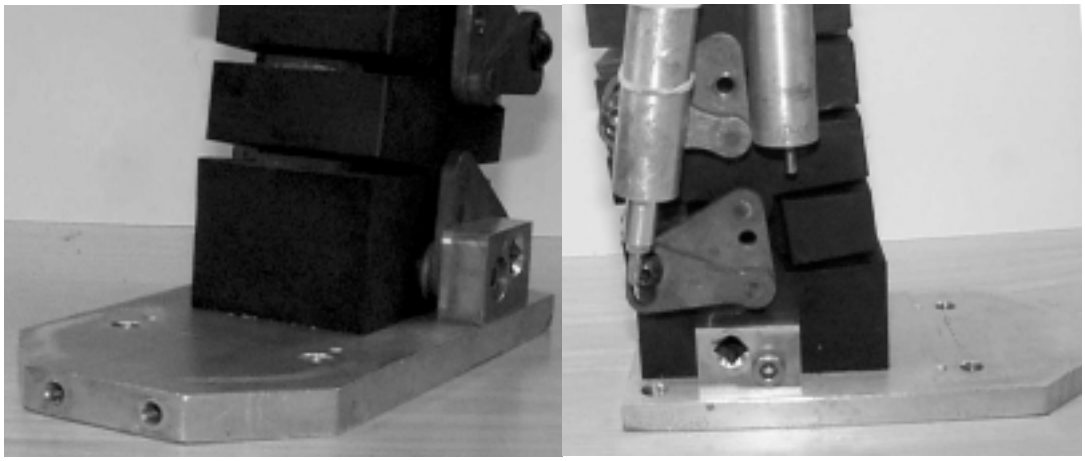

Figure 19. L5 – pelvis interface and H-point position indicator (left oblique and right side).

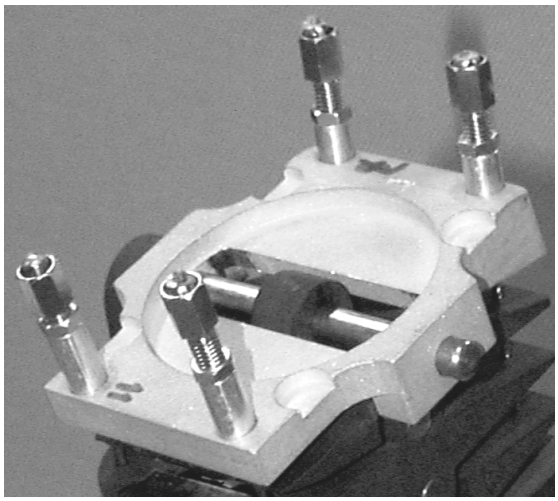

Figure 20. Occipital interface with neck muscle substitute adjustments.

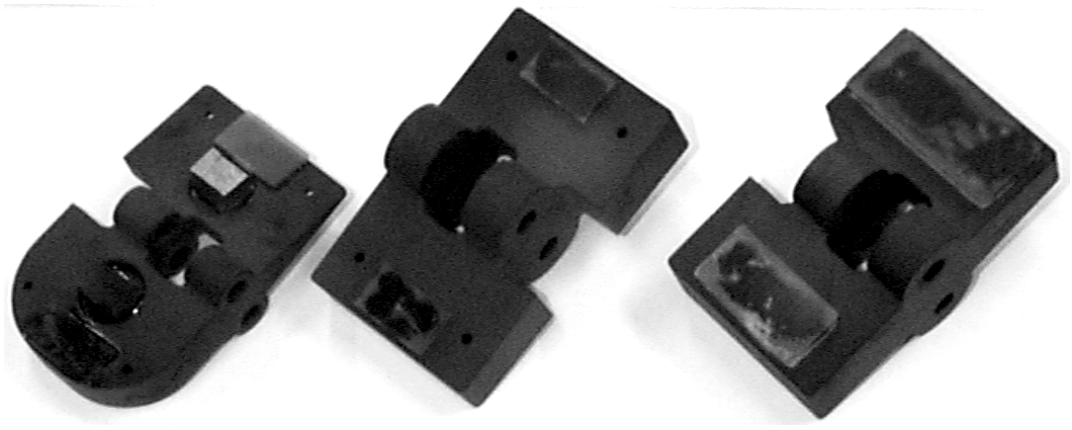

Figure 21. Cervical, thoracic and lumbar vertebrae with mounted rubber bumpers.

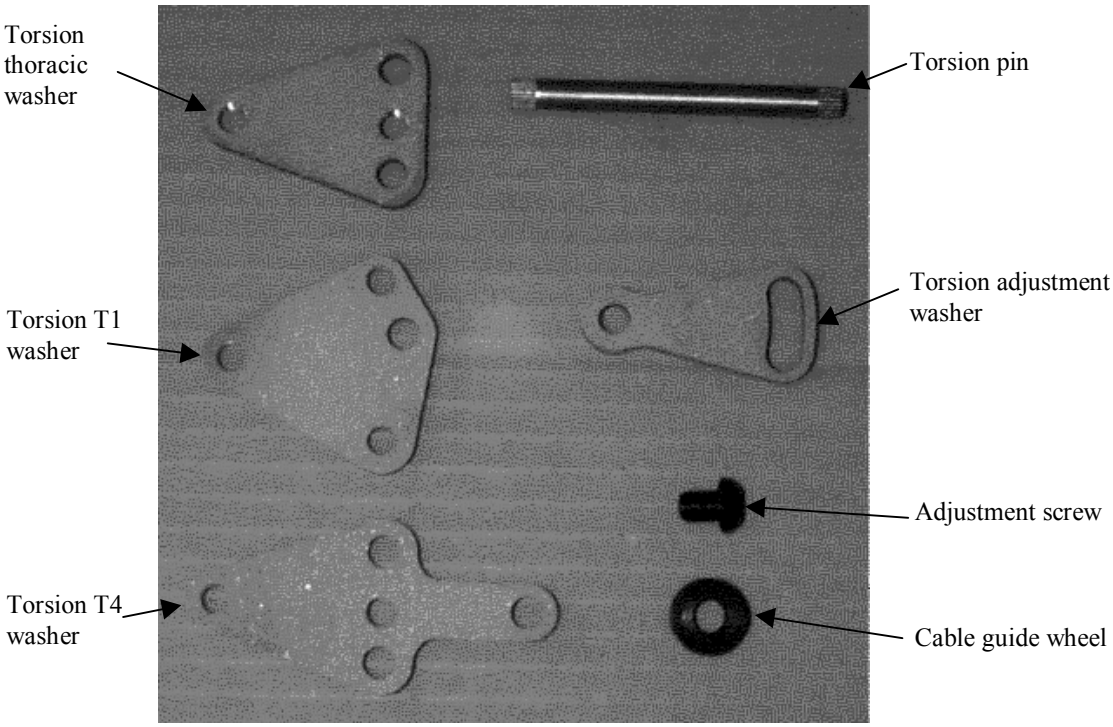

Figure 22. Torsion pin, washers, cable guide wheel and adjustment screw.

Assembly instructions - To glue the rubber bumpers into the vertebrae (size according to Appendix A and Figure 21):

- Remove any excessive glue from the vertebrae.
- Wash the vertebrae with mild detergent.
- Apply primer (Sverotec-3) to the bumper and vertebrae surfaces.
- Draw a line onto the thoracic and lumbar vertebrae top surfaces. The line should be parallel with the anterior and posterior surfaces and shifted 2 mm to the center of the vertebrae.
- Apply glue (Loctite 406) to one of the surfaces of the rubber bumper and press the bumper gently onto the vertebra. The cervical bumpers should be positioned in the center of the countersink. The lumbar and thoracic bumpers should have their anterior/posterior surfaces aligned with the line.

To assemble or disassemble the lumbar and thoracic spine:

- Screw the S1 vertebra onto the pelvis interface (Figure 19).
- Apply glue (Loctite 270) to one of the spline surfaces on all of the torsion pins and insert the torsion pins into lumbar, thoracic and T4 torsion washers (the pins should have a different mounting direction on washers that are to be mounted on the right and left side of the spine).
- Fit one of the lumbar vertebrae on top of the S1 vertebra. Insert the torsion pin/lumbar torsion washer unit into the joint.
- Screw the torsion washer and the H-point position indicator onto the S1 vertebra (Figure 19). Place the spacer washer between the torsion washer and the S1.
- Fit next vertebrae and insert the torsion pin/torsion washer unit into the spine joint and continue until the thoracic and lumbar spine is completed (Figure 30 and

Figure 31). At T4 there should be a shim washer placed between the torsion washer and the vertebra.
- Glue and fasten the torsion adjustment washers to the torsion pins. Note that the adjustment washer may be flipped in order get the adjustment mark closer to the middle of the torsion adjustment washer marker scale). The adjustment screw should preferably be in the middle of the adjustment range on the torsion adjustment washer.
- Attach all adjustment screws.
- Fit one of the cervical vertebrae on top of the T1. Insert the T1-C7 joint pin and secure with two nuts on each side (Figure 32).
- Fit the rest of the cervical vertebrae and insert neck joint pins.
- Screw the other H-point position indicator attachment onto the right side of the S1 vertebra (Figure 19).
- Fit the occipital interface and insert the C1-occipital joint pin.

3.2 Damper

Inherent parts – Below is a list of all parts of the damper. ():
Paddle wheel (1 unit).
Body (1 unit).
Cover (1 unit).
Washer (1 unit).
Roller bearing, lateral (1 unit, SKF 61801).
Roller bearing, central (1 unit, SKF 618/8).
Screws and nuts (20 each, M2*15).
Valve screw (2 units, M4*4).
Cable attachment screw (1 unit, M3*10).
Oil (Meropa 680).
Mounting screw (1 unit, M8*12).
Rubber seal (SKF ORX 21.95*1.78).

Figure 23. Damper parts, seal and damper oil in a syringe.

Assembly instructions – Assembly of the rotational damper (assembly parts in the order from left to right, Figure 24):

- Press (force fit) the lateral roller bearing (1 unit, SKF 61801) onto the shaft of the damper paddle wheel shaft. The distance between the side of the roller bearing and the top of the bearing shaft of the paddle wheel should be more than 0.1 mm. The roller bearing should however not be in contact with the paddle (Figure 25).
- Press (force fit) the central roller bearing (1 unit, SKF 618/8) onto the damper cover shaft. The distance between the side of the roller bearing and the base of the damper cover shaft should be approximately 0.1 mm.
- Fit the damper paddle wheel on the damper lid.
- Visual check of the clearance between the surfaces of the damper body and the paddle wheel.
- Apply a thin layer of "Golden Hermitite" seal on the surface of the damper body that will be in contact with the damper lid. The less seal inside the damper the better.
- Mount the damper cover onto the damper body by the use of four screws that are evenly distributed along its rim.
- Check the paddle wheel clearance. The paddle wheel must not contact the damper body surfaces anywhere along its path. If the clearance is not acceptable, move the damper cover relative the damper body.
- When the clearance is acceptable, mount the rest of the screws. Check the clearance between the damper body and the paddle wheel once more.
- Apply Meropa oil onto the rubber seal and place the rubber seal in the groove in the damper body.
- Apply a thin layer of "Golden Hermitite" seal onto the shaft of the paddle wheel.
- Press the washer onto the damper paddle wheel shaft and secure with a screw and nut (Figure 28). The fitting should be force fit.
- Screw a valve screw (socket head cap screw, M4) into the damper body and a second screw on top of the first screw (countersunk, reduced the head ∅*height to 5*2.2 mm, M4) in order to seal the damper adjustment.
- Fill Meropa oil into the damper. Position the paddle wheel according to Figure 26 and Figure 27. It is vital that there is no air entrapped inside the damper. It must be full of oil! In order to get all air out of the damper it may be necessary to heat the damper/oil unit and to repeatedly cycle the paddle wheel. In order to check if there still is air entrapped in the damper, turn the paddle wheel back and forth and check the oil level in the filler neck. The oil level in the filler neck should be constant if the damper is full, while the oil level usually is not constant when there is air entrapped inside the damper.
- Mount the filler cap (counter screw with reduced head height, M3)
- Mount the cable attachment screw.

Comment: The key to successful assembly of the damper unit is tight fitting between the central roller bearing and the cover shaft as well as between the lateral roller bearing and the paddle wheel shaft.

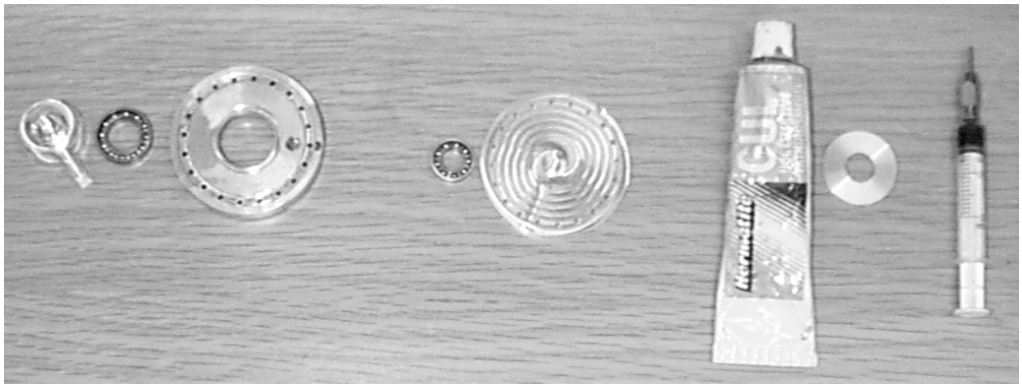

Figure 24. Damper parts in assembly order.

Figure 25. Paddle wheel, central roller bearing and washer.

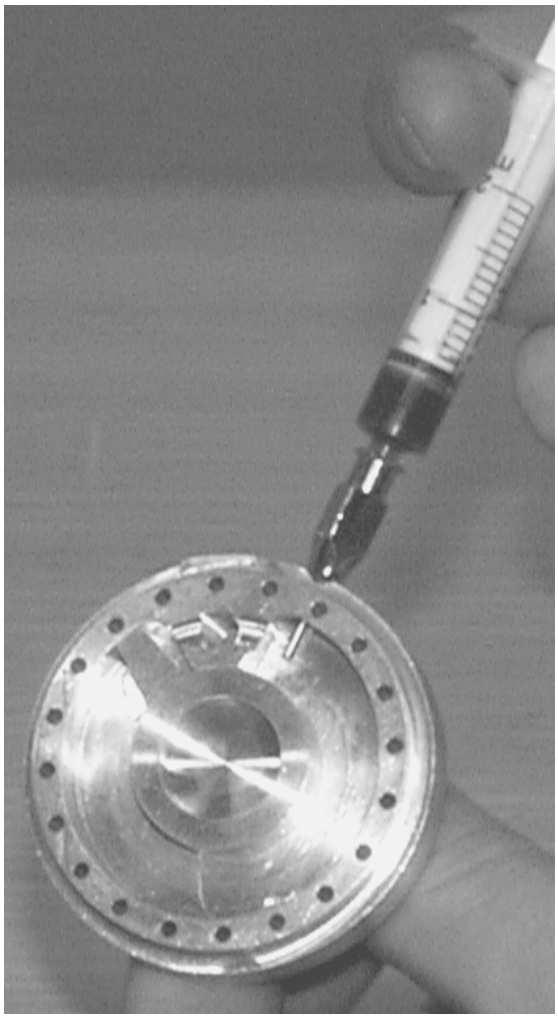

Figure 26. First filling of damper.

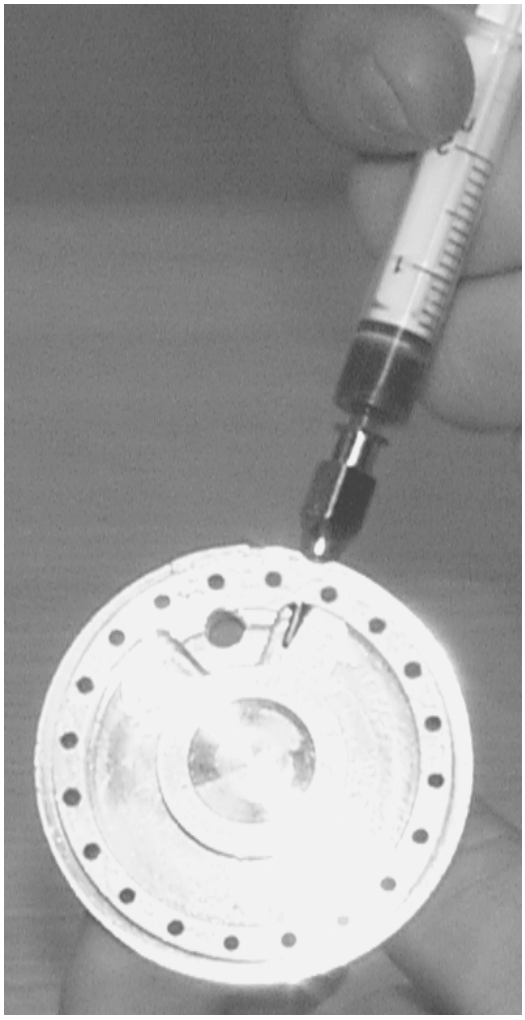

Figure 27. Second filling of damper.

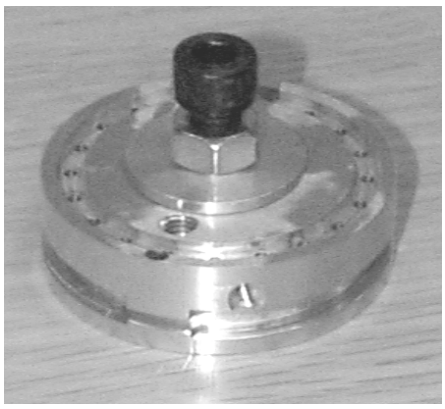

Figure 28. Temporary mounting of the damper washer onto the damper wheel shaft by the use of M8 screw and nut.

3.3 Muscle substitutes

Inherent parts - Below is a list of all parts of the muscle substitutes (Figure 29):
Damper (1 unit).
Damper mounting screw, hexagonal screw (1 piece, MC6S, M8*10).
Spring (2 pieces).

Spring arrangements (2 units).
Spring adjustment screw and nut (2*2 pieces).
Cable (1 piece) to be used in the right side muscle substitute system (damper loaded).
Cable (2 pieces) to be used in the left side muscle substitute system (spring loaded).
Cable house (2 pieces).
Cable adjustments screw (4 pieces).
Cable adjustments attachment (4 pieces).
Cable guide wheel (1 piece).
Terminal (4+2 pieces).

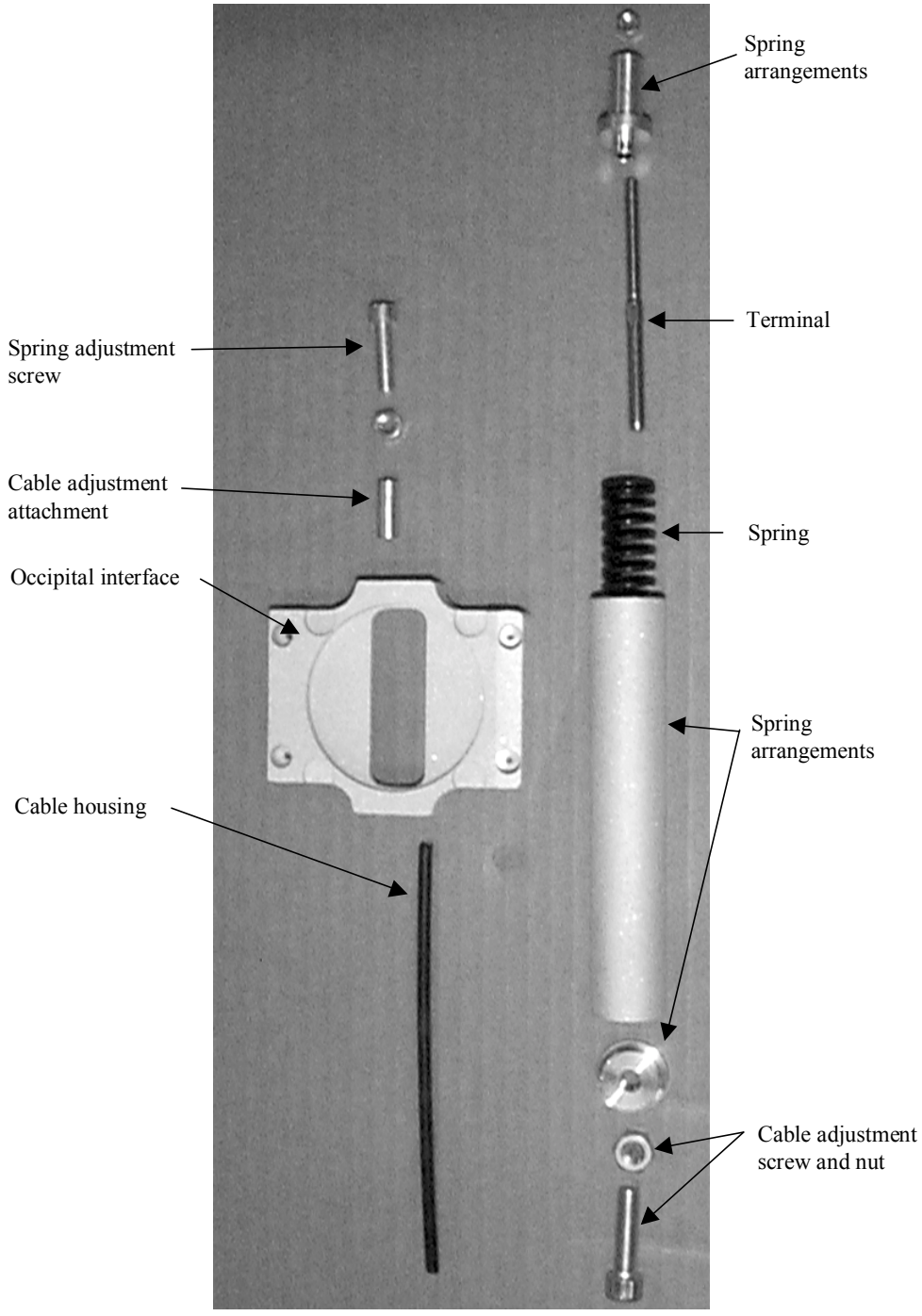

Figure 29. Close up view of spring loaded muscle substitute parts.

Figure 30. Left side view of the spine.

Figure 31. Right side view of the spine.

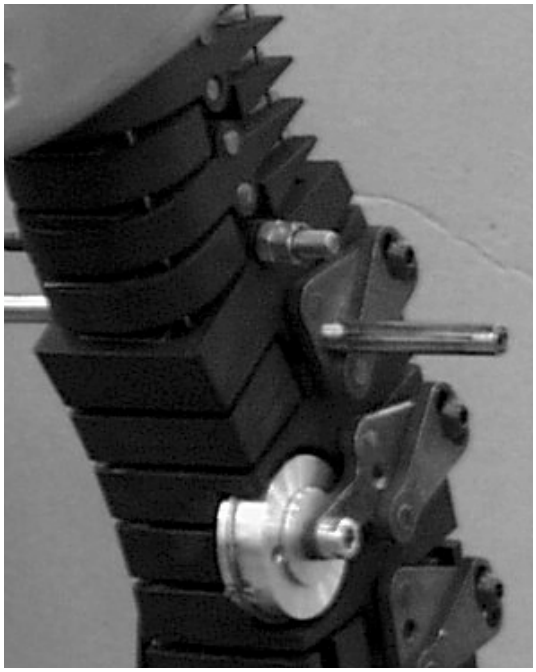

Figure 32. Oblique view of left side of the spine from T5 to C4.

Assembly instructions - Mounting the damper loaded muscle substitutes (Figure 29, Figure 30, and Figure 32):

- Attach the damper unit to the T4 torsion washer with the damper mounting screw (this could be done before or after the cable is installed).
- Glue (Loctite 270) the adjustment attachment to the occipital interface.
- Thread the cable through the cable adjustment screw, and pass it through the cable adjustment attachment on the right side of the anterior of the occipital interface.
- Thread the cable through the hole on the right side of the anterior of the C1 to T3 vertebrae.
- Wrap the cable clockwise around the damper unit (Figure 33).
- Thread the cable through the hole on the right side of the posterior of the T3 to C1 vertebrae (the cable should run counter clockwise around the cable guide wheel).
- Thread the cable through the cable adjustment attachment on the right side of the posterior of the occipital interface and pass it through the adjustment screw.
- Attach the cable to the damper by tightening the cable attachment screw.
- Adjust the neck curvature to initial posture.
- Make sure the cable adjustment screws are in the middle position.
- Attach the cable terminals on to the cable ends (both ends, there should be no slack).
- Refill the damper with oil, as there may be air bubbles in the damper unit.
- Adjust the cable pre-tension.

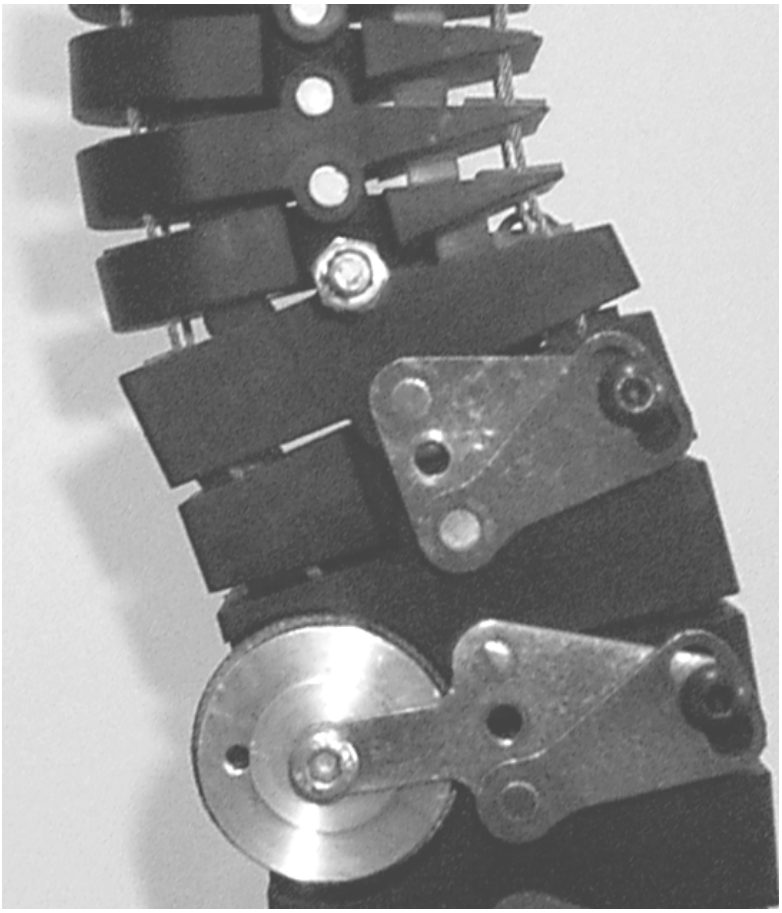

Figure 33. View of damper and cable.

To mount the spring loaded muscle substitutes (Figure 29 and Figure 31):
- Mount a spring arrangement adjustment nut onto the end of an elastic muscle substitute cable.
- The posterior elastic muscle substitute cable should be threaded through the longest spring, the spring arrangement assembly, the spring adjustment nut and screw and the cable housing.
- Continue to thread the cable through the left posterior holes in the T3, T2, T1 and C7 to C1.
- Thread the cable through the cable adjustment attachment in the occipital interface and finally through a cable adjustment screw.
- Attach a cable terminal to the cable (there should be some slack in order to adjust the initial head position, initial neck curvature and to unload the muscle substitutes and neck rubber bumpers when the dummy is stored).
- The anterior elastic muscle substitutes should be mounted similarly to the posterior muscle substitute.
- Pre-tense the elastic muscle substitutes a total of 14 mm (the posterior and anterior muscle substitute will not shorten the equal amount).

3.4 Shoulder yoke

Inherent parts - Below is a list of all parts necessary for the installation of the shoulder yokes:
Torso.
Shoulders yokes (2 pieces, Figure 34).

Hybrid III shoulder yoke screws (2 pieces, Figure 34).

Figure 34. Shoulder yoke assembly.

Assembly instructions - Lubricate the shoulder joint surfaces with grease, insert the shoulder into the arm attachment, and mount the arm attachment screws. The arm attachment screws should be tightened according to section 2.2. Use a socket key (3/16'') when adjusting the shoulder torque (Figure 34).

3.5 Pelvis interface - abdomen attachment

Inherent parts - Below is a list of parts used to assemble the pelvis interface abdomen attachment onto the torso:
Torso.
Pelvis interface/abdomen attachment (1 piece).
Pelvis interface/abdomen attachment screws, countersunk hexagonal screws (2 pieces, MF6S M6x8).

Assembly instructions - Place the torso with the abdomen facing down.
Mount the pelvis interface/abdomen attachment the bottom of the torso using the attachment screws.

3.6 Torso - spine attachments

Inherent parts - Below is a list of parts used to attach the torso to the spine:
Assembled spine (se section 3.1).
Torso.
Spine-torso interface pins (15 pieces, Table 8 and Figure 35).
Spacers (diameter 10mm, 3 units length 30mm and 3 units length 35mm).
Pelvis position indicator attachment (1 piece).
Pelvis position indicator attachment screws (2 pieces, M6*25).

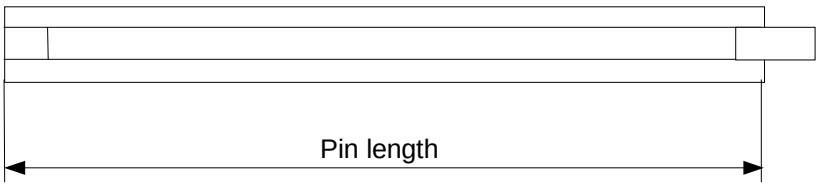

Figure 35. Spine-torso interface pins.

Table 8. Spine-torso interface pin length

Pin	L1	L2	L3	L4	L5	L6	L7	L8	R1	R2	R3	R4	R5	R6	R7
Pin length	50	50	84	115	125	125	125	132	50	50	107	120	125	120	125

(distance according to Figure 13, L=left, R=right, pin 1 at the top and pin 7 and 8 respectively at the bottom of the torso).

Assembly instructions - Place the torso with the abdomen facing down. Place the spine in the curved rectangular container inside the torso and fit the pelvis interface/abdomen attachment in the slit in the S1 front. Attach the pelvis indicator attachment (the "pelvis interface abdomen attachment" is then also secured). Place the spine-torso interface pins in the holes in the torso (15 pieces). The pins are arranged according to table 1. The prefix of the number represent left side (L) and right side (R) respectively. The numbers are in order from top to bottom, e.g. R1 is located next to the right shoulder.
Thread the spacers on every third spine-torso interface pin on both sides. Start at the top (L1, L4 etc). Use the shorter (30 mm) in the thoracic spine and the shorter (30 mm) spacers in the lumbar spine.
Screw the spine-torso interface pins into the threaded holes in the torsion washers. The lowest holes are not to be used.

3.7 Pelvis interface – pelvis attachment

Inherent parts - Below is a list of parts used to attach the pelvis interface to the pelvis:
Assembled torso and spine.
Modified Hybrid III pelvis (Figure 36 and Figure 37).
Pelvis attachment screws (hexagonal screws, MC6S, 2*M10*30 and 2*Hybrid III standard pelvis attachments screws (long model).

Assembly instructions - Connect the pelvis to the pelvis interface with three M10 screws.

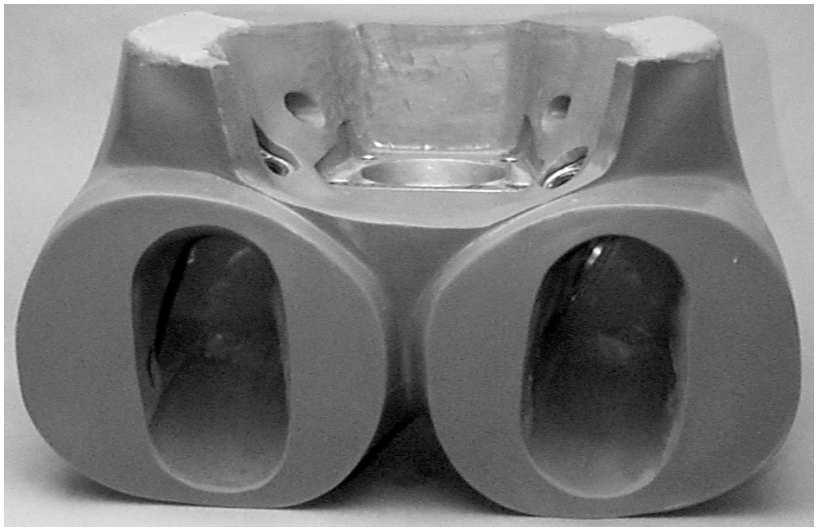

Figure 36. Modified Hybrid III pelvis, front view.

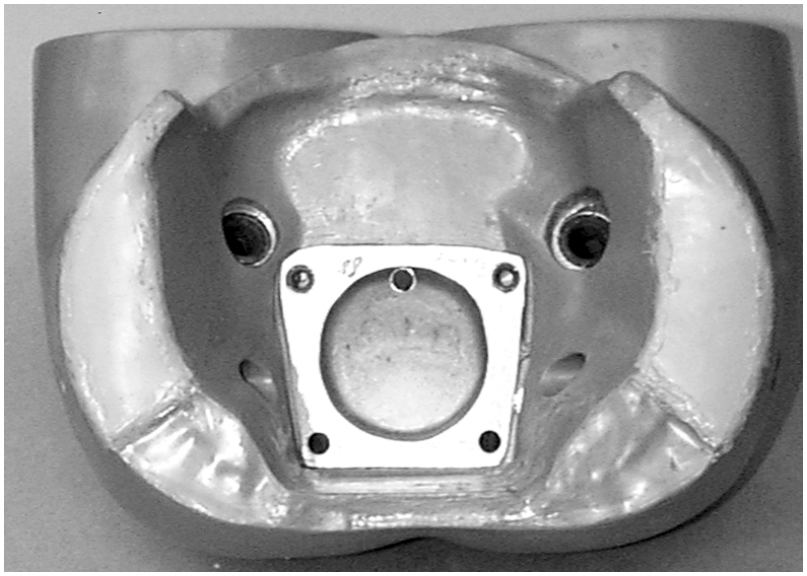

Figure 37. Modified Hybrid III pelvis, top view.

3.8 Back support – torso attachment

Inherent parts - Below is a list of parts used to attach the back support to the torso:
Torso.
Teflon sheet.
Foam plate.

Assembly instructions - Glue the Teflon sheet to the foam plate. The foam plate should be centered on the sheet. Place the sheet/foam plate in the back of the spine compartment. The Teflon sheet should face the vertebrae. Close the left and right spine compartment cover over the back plate and join the edges by sewing or gluing (Wacker RT623 silicon A+B).

3.9 Clothing

In order to achieve friction between the dummy and the seat that best approximates friction experienced by humans (between clothing and the bones), the BioRID should be clothed in double layers of Lycra. One set of Lycra clothing is black and one is colored. The cloths have one smooth and one mat side. Place the smooth sides against each other so that the seams face inwards.

4 Adjustments of BioRID II

This chapter describes the spine, pelvis, shoulder and femur joint adjustments.

4.1 Spine curvature

The angle of every thoracic and lumbar spine joint can be adjusted individually. Default thoracic and lumbar spine sitting posture is obtained when the joints are adjusted in such a way that the marker at the torsion adjustment washers and the marker at the torsion washers are in line. The angle between two thoracic or lumbar vertebrae can be adjusted (1 deg./marker) after the locking screw has been released (Figure 38). Tighten the torsion adjustment screws with a torque of 15-Nm. Approximate default cervical spine sitting posture should be obtained by adjusting the muscle substitutes and upper thoracic spine curvature properly. The dummy should be stored with the spine in the position of normal curvature in order to avoid excessive load on the rubber blocks between the vertebrae.

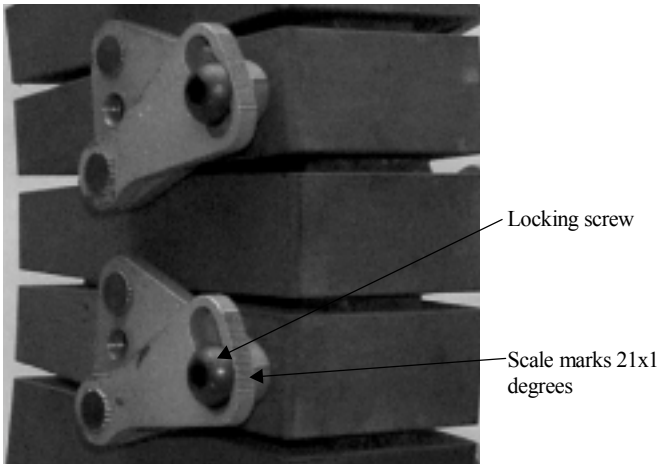

Figure 38 Thoracic and lumbar spine joints

Default lumbar spine curvature - Default sitting posture is achieved by adjusting the lumbar spine as follows:
Straighten the lumbar vertebrae until they are aligned in a straight line (Figure 39). Tighten the torsion adjustment screws with a torque of 15-Nm. Adjust the L5-S1 joint such that the distance between L5 and S1 is the same as between the other lumbar vertebrae.

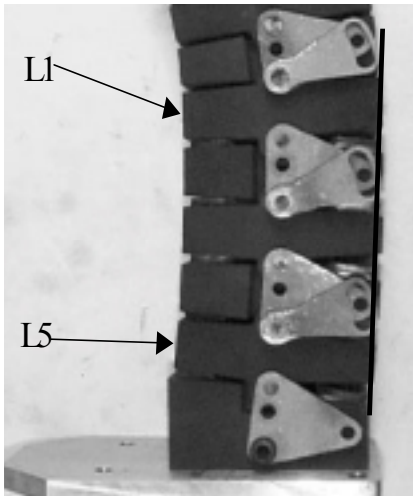

Figure 39. Default adjustment of the lumbar spine.

Default thoracic spine curvature - Default sitting posture is achieved by adjusting the thoracic spine as follows:
Adjust all the joints in the thoracic spine to obtain equal range of motion forward and rearward, i.e. so that the distances between the vertebrae are similar posterior and anterior. Tighten the torsion adjustment screws with a torque of 15-Nm.

Default cervical spine posture - The BioRID neck curvature is at default position when the cervical joint centers are located at an imaginary arc with a radius of 190 mm (Figure 40). The dummy sitting angle (due to the effect of gravity acting on the head), neck muscle substitute pre-tension and the inter-vertebrae rubber bumpers determine the cervical spine curvature. To achieve default neck spine curvature, adjust the spring-loaded part of the muscle substitute system. An alternative way to adjust the default neck curvature would be; first adjust the lumbar spine, the S1 to lumbar spine and the thoracic spine; then tune the neck elastic muscle substitute length until the angle between the pelvis interface and the head base is 26.5 degree (Figure 40).
Cervical spine curvature adjustments are also presented in Section 6.3.

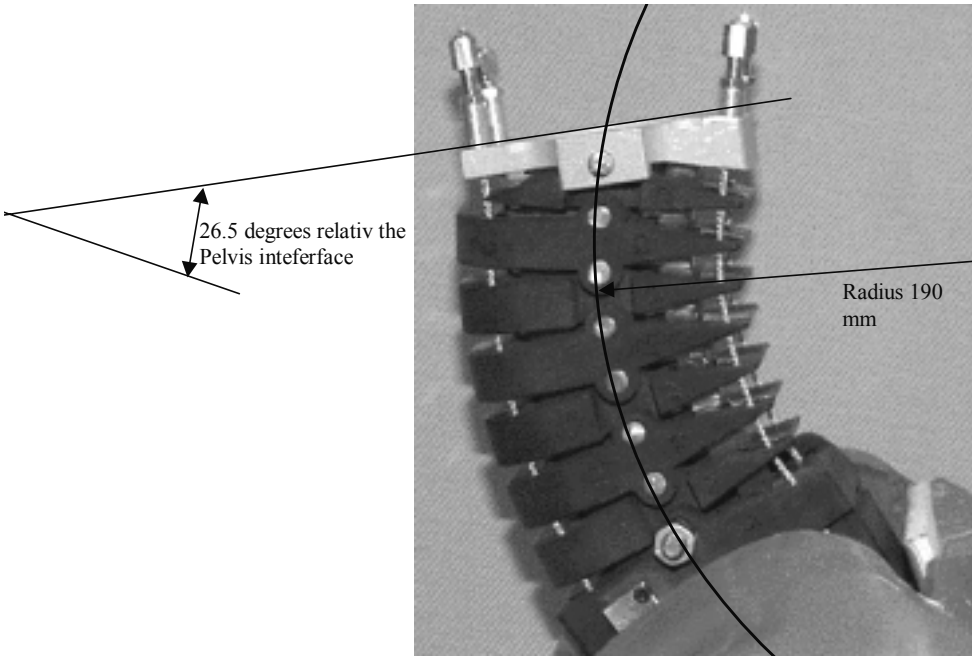

Figure 40. Default cervical spine curvature.

Adjusting the cable pair on the right side of the dummy changes the neck curvature. The anterior and the posterior cables are shortened and lengthened, respectively. The cable pre-tension affects the friction and the resistance to flexion/extension of the neck, which influence the response of the dummy. Be sure to keep proper pre-tension of the springs. The cable pre-tension can be adjusted either in the occipital interface, at the spring arrangements or at the end of the springs.

Adjusting the cable pair on the left side of the dummy does not change the neck curvature. However, the pre-tension affects the muscle substitute system friction. Avoid excessive load on the damper and the cable system by shortening the cable until there is no play. Do not tighten too hard. The damper cable pre-tension can only be adjusted at the occipital interface.

4.2 Shoulder yoke to arm attachment joint torque

Adjust the default shoulder yoke to arm attachment joint torque to approximately 8-Nm (Figure 41) as follows:

- Position the dummy in erect seating posture.
- Set the elbow angle to 90 degrees.
- Hold the arm horizontal. The upper arm (above the elbow) should point forward and the lower arm (below the elbow) should point inward.
- Tighten the arm attachment screw so that the arms almost rotate downward as a result of the gravity.

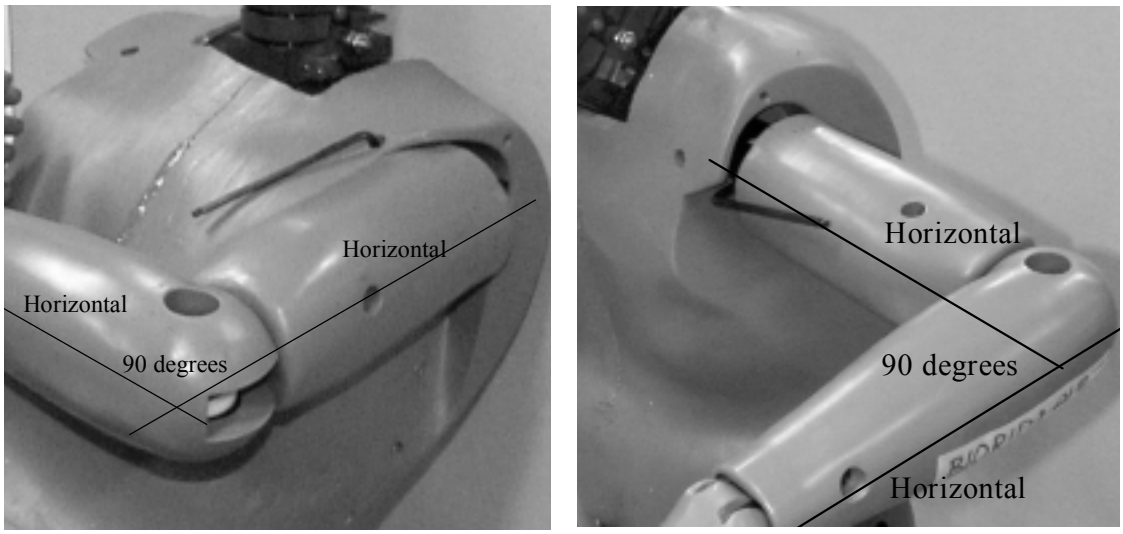

Figure 41. Shoulder yoke and upper arm to shoulder yoke joint torque adjustment.

4.3 Upper arm to shoulder yoke joint torque

Adjust the default upper arm to shoulder yoke joint torque to approximately 8-Nm as follows:

- Position the dummy in erect seating posture.
- Set the elbow angle to 90 degrees (Figure 41).
- Hold the arm so that the upper arm is horizontal and the lower arm is vertical. The upper arms should point in the lateral direction and the lower arms should point forward.
- Tighten the shoulder yoke screws so that the arms almost rotate downward due to gravity.

4.4 Femur joint torque

The BioRID I and P3 were validated with a low femur joint torque of approximately 30-Nm in flexion and extension. To adjust the initial femur joint torque to approximately 30-Nm:

- Dismount the rubber torso from the spine and pelvis interface.
- Position the dummy in erect seating posture (on its posterior part of the pelvis on a table).
- Remove lower leg and foot.
- Hold the upper legs horizontal.
- Tighten the femur joint adjustment screws so that the upper legs almost rotate downward due to gravity.

5 Instrumentation

5.1 Sensor requirements, positions and classes

The sensor position, measurement range and channel class recommendations are presented in Table 9 and Figure 42. An alternative position for the T1 accelerometer is on the T1 position indicator. For this alternative position the initial x-axis is horizontal and the z-axis is vertical relative inertia.

Table 9. Sensor position, measuring range and filter recommendations.

Location	Direction	Measure	Range (g)	Comments	SAE J211 Channel class
Head	x	Acc	100-500	H3 standard	1000
	y	Acc	60	H3 standard	1000
	z	Acc	100-500	H3 standard	1000
Head	Ang.	Acc	-	Optional	1000
Upper neck	3-ax	Forces	High resolution	Modified Denton	1000
Upper neck	3-ax	Moments	High resolution	Modified Denton	600
C4	x	Acc	50-200	Parallel with the vertebra center line	18
	z	Acc	50-200	Orthogonal with the vertebra center line	18
T1	x	Acc	50-200	Parallel with the vertebra center line	18
	z	Acc	50-200	Orthogonal with the vertebra center line	18
T8	x	Acc	50-200	Parallel with the vertebra center line	18
	z	Acc	50-200	Orthogonal with the vertebra center line	18
L1	x	Acc	50-200	Parallel with the vertebra center line	18
	z	Acc	50-200	Orthogonal with the vertebra center line	18
Pelvis	x	Acc	50-200	H3 standard	1000
	y	Acc	50-200	H3 standard	1000
	z	Acc	50-200	H3 standard	1000
Pelvis	Angular	Acc	-	Optional	1000

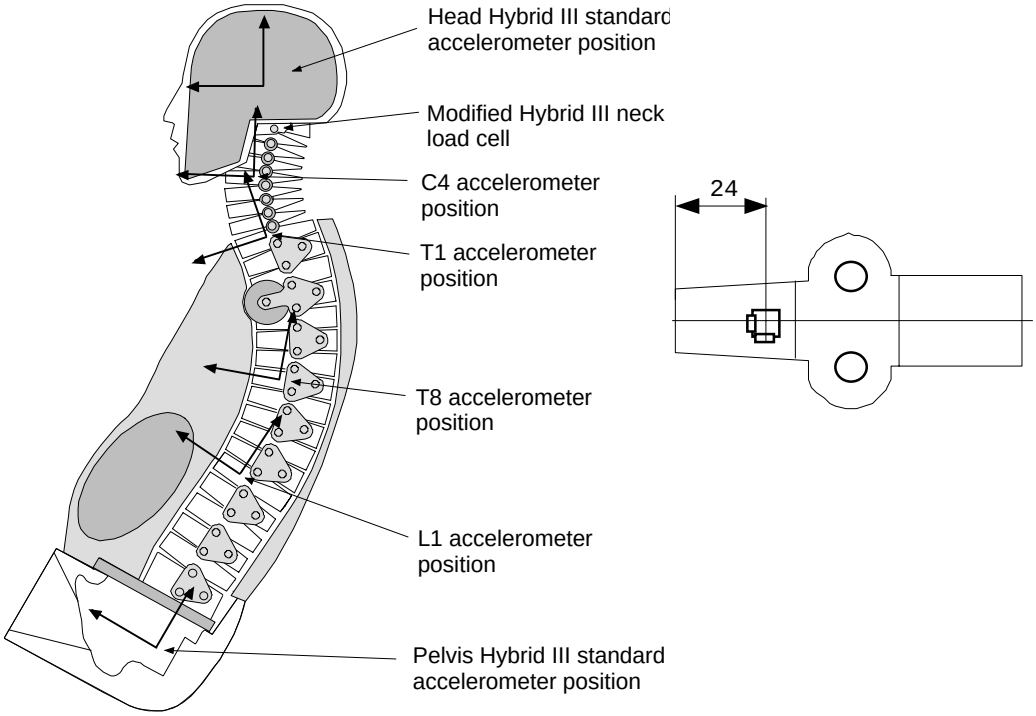

Figure 42. Instrumentation positions and measuring directions.

5.2 H-point position indicator

The Hybrid III H-point indicator fits the H-point indicator attachment on the BioRID pelvis interface (Figure 19). The BioRID II and Hybrid III H-point attachments are located at the same distances and angles relative the H-points. The H-point position indicator top surface is parallel with the pelvis mounting surface/pelvis interface bottom surface.

The H-point position may be estimated from the H-point position indicator. The indicator should be mounted to the H-point position indicator attachment, which should be mounted to the pelvis interface (Figure 43).

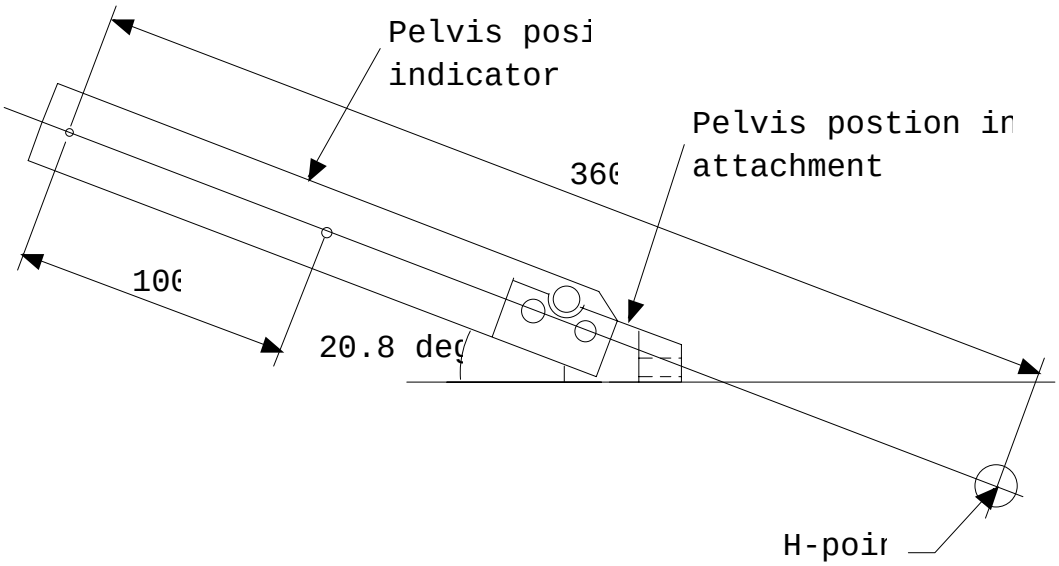

Figure 43. Distances between the H-point and pelvis position indicator.

5.3 T1 position indicator

The T1 center of rotation is not visible during a normal sled test. Therefore, a T1 position indicator may be attached to the T1-C7 joint pin (Figure 44).

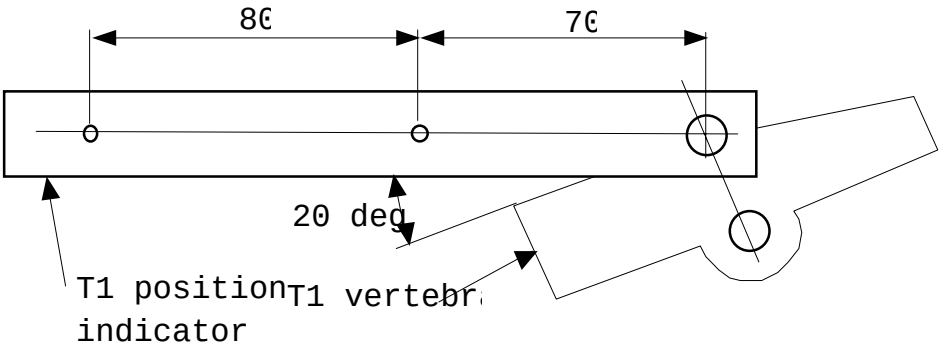

Figure 44. Distances between the T1center of rotation and T1 position indicator.

5.4 Calculation of moment about the Occipital Condyle

The neck load cells used in BioRID measure moments about the Y axe. The Y axe of the load cell is displaced from the axes of the occipital condyle. Independent of the reported filter class of the force data, its filter class must be adjusted to be consistent with the moment data prior to attempting this calculation. To calculate the moments about the occipital condyle, Equation 1 should be used.

$$Mocy = My - D * Fx \qquad \text{Equation 1}$$

where

Mocy	Moment Y about the occipital condyle.
Fx	Load cell force output in the X direction in Newton.
D	Distance between the axis of the load cell and the axis of the condyle. For the BioRID II Upper Neck Load Cell (Denton 2564 three channel neck load cell) the distance is 0.01778 m.

The sign convention in SAE J1733 is to be used.

6 Biofidelity, repeatability and durability

6.1 Biofidelity

BioRID II is validated for a rear impact in the range of ΔV=7 to 15 km. Comparisons between human volunteer response, cadaver response and the BioRID response are found in a number of publications, see chapter 13.

6.2 Repeatability

Evaluation of dummy repeatability is found in chapter 1.4, Davidsson et al. 1999 IRCOBI, and Davidsson et al. 1999 STAPP.

A BioRID I was exposed to repeated ΔV=17 km/h rear impacts in seats from a standard mid-size car model intended for the European market was carried out at Autoliv Research (Boström et al., 2000 *Accident Analysis and Prevention,* Vol. 32, pp. 321-328). The BioRID I instrumentation data was digitized at 10 kHz and digitally filtered according to SAE J211 (upper neck loads CFC1000, sled acceleration CFC60, head CFC1000, lower neck CFC180 and pelvis CFC1000). After filtering lower neck (T1) x- and z-, head z-, and pelvis z-accelerometer data was smoothed (window size ±60). The sled, head, and pelvis x-acceleration and upper neck load cell data was not smoothed. An analysis of variance was used to calculate coefficients of variation (C.V.) for repeatability. The C.V. is a measure of variability expressed as a percentage of mean peak value defined below.

Repeatability: $$C.V. = \left[\frac{S.D.}{mean}\right] * 100\%$$

The C.V. of 5% or less is considered good and a C.V. of 10% or less is considered acceptable (Wismans et al. (1994). The C.V. for the BioRID I neck axial load was too large but could have been due to variations of the physical properties and the adjustments of the head restraint in the test which resulted in very low upper neck axial load relative the other tests. The C.V. for pelvis, lower neck and head z-accelerations were acceptable and the x-acceleration was good (Table 10).

Table 10. Coefficient of variation, BioRID I tested in standard car seats (n=5).

Parameter:	Mean	S.D.	C.V. (%)
Sled acceleration (m/s^2)	104	1.1	1.0
Lower neck x-acceleration (m/s^2), first peak	116	4.0	3.4
Lower neck x-acceleration (m/s^2), second peak	152	11.5	7.6
Lower neck z-acceleration (m/s^2), first positive peak	4	3.1	7.1
Lower neck z-acceleration (m/s^2), first negative peak	-14	1.1	7.8
Head x-acceleration (m/s^2)	283	13.0	4.6
Pelvis x-acceleration (m/s^2)	165	3.6	2.2
Head z-acceleration (m/s^2), first positive peak	102	10.9	10.8
Head z-acceleration (m/s^2), first negative peak	-16	0.8	4.9
Pelvis z-acceleration (m/s^2)	60	3.7	6.2
Upper neck shear load (N), first negative peak	-455	45.9	10.1
Upper neck axial load (N)	2900	817.0	28.1

6.3 Durability

The BioRID P3 has been shown to withstand rear impacts of ΔV=28 km/h and 15 g in conventional car seats with head restraints in normal and lowest position (hyper extension was avoided). It has also withstood tests in rigid seats with a ΔV=20 km/h and out-of-position tests (large gap between head and head restraint) with a ΔV=15 km/h in conventional seats with head restraints.
The dummy will most likely withstand frontal impacts of ΔV=20 km/h.
Oblique frontal impacts and side impacts should be avoided.

7 Initial posture

It is recommended that the BioRID II be used in a pure rear impact (180 degrees) with normal sitting postures, using conventional car seats with head restraints.

7.1 Initial pelvis position and pelvis angle

Neither the initial BioRID II pelvis angle nor the H-point position has to be that of the Hybrid III. The default pelvis angle is 26.5 degrees and the head base should then be horizontal (if the spine curvature is default). In a volunteer seat posture study it was shown that the average volunteer pelvis was tilted backwards (extension) more than the BioRID P3 and Hybrid III pelvis (Cruickshank and Couper, Division of Traffic Safety, Chalmers, 1999). In another study (Davidsson et al, STAPP, 1999) it was concluded that the BioRID P3 iliac crest horizontal displacements (for two types of test seats) were smaller than that of the average volunteer. This occurred although most of the volunteers had pelvis to seatback contact prior to impact. Do not position the dummy with the H-point to far aft in the seat.

7.2 Initial torso shape

The BioRID II back shape and spine curvature resembles that of an average driving 50%ile male seated in standard US market bucket seats from the early 80's (Schneider et al, 1983). In that report, it was concluded that the human lumbar spine is straight, the thoracic spine has a kyphosis and the cervical spine has a lordosis. Even though seats of today have different shape and stiffness compared to those included in the UMTRI-study, the posture of the average 50% male driver has not changed significantly. However, it is possible to change the spine curvature and back surface shape by adjusting the angles between the vertebrae in the thoracic and lumbar spine.

7.3 Initial head position

There are at least three possible choices of initial head position:

- Adjust the cervical spine curvature according to the instruction in section 4.1.
- Place the dummy in desired position. Adjust spine until head is horizontal.
- Place the dummy in the desired position. Adjust the cervical spine until the desired distance between the head and the head restraint is achieved.

Adjusting the cable pair on the right side of the dummy changes the neck curvature. The anterior and the posterior cables are shortened and lengthening, respectively. The cable pre-tension affects the friction and the resistance to flexion/extension of the neck, which influences the response of the dummy. Be sure to keep proper pre-tension on the springs, see further details in chapter 4. The cable pre-tension can be adjusted either in the occipital interface or at the spring arrangements.

7.4 Out-of-position test

The BioRID II may be used in out-of-position tests (test where the dummy is leaning forward prior to test). There are at least two possible methods of positioning the BioRID II for a leaning forward out-of-position test:

1. Change the lumbar and thoracic pre-impact spine curvature by flexing the joints. The BioRID II will then resemble a human who is trying to reach forward.
2. Tilt the BioRID forward (flexion of the femur joints). This pre-impact posture resembles that of a human who has rotated forward due to braking.

8 Calibration of BioRID II

It is recommended that the BioRID II is calibrated/checked after 20 conventional tests, using a spine and torso evaluation test. The dummy should also be checked after each abnormal test (e.g. after excessive seatback backward rotation). Before the muscle substitute system is assembled, a damper calibration test should be carried out.

8.1 Spine and torso evaluation test

The objective of this test is to measure the response of the BioRID neck in the extension phase.

Materials and Method - The BioRID II should be fitted with shoulder yokes, modified Hybrid III head, upper neck load cell, foam and Teflon foil between the back of the spine and silicon rubber, and the abdomen bladder should be filled with water. The dummy should, however, not be fitted with pelvis, lower extremities or upper extremities.

The pelvis interface should be attached to the calibration rig attachment (Figure 45). The calibration rig should be placed on a sliding table covered with a foil of Teflon. The calibration rig drawings are provided in Appendix I (made in tubes with the dimensions 50*50*2 mm). Temperature: 22±3deg C. Relative humidity 40±30%.

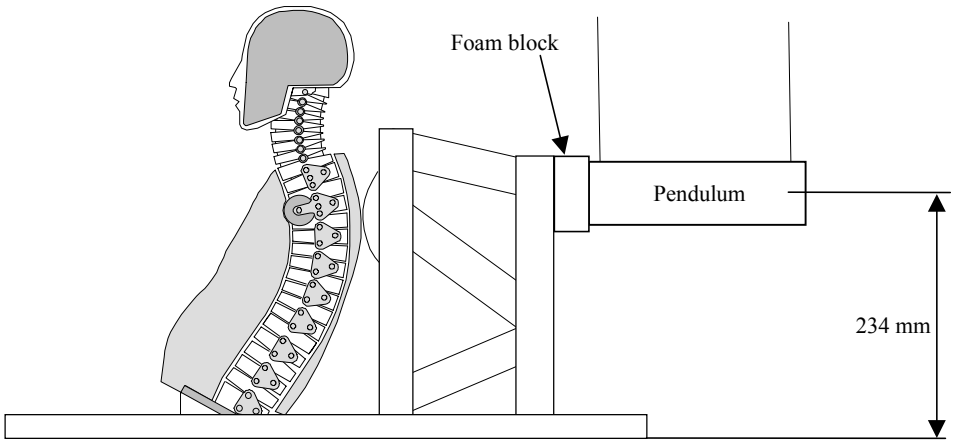

Figure 45. Test set up of spine and torso evaluation test.

Hit the fixture/padding at a height of 234 mm above the bottom of the rig base with a pendulum to achieve the sled/calibration rig pulse specified in Table 11 and velocity profile as specified in Table 14. Suggestions of pendulum, padding and sled characteristics to obtain the specified corridor are provided in Table 11.

Table 11. Pendulum, padding and sled data.

Parameter	**Specification**
Pendulum mass	33,4 kg
Pendulum diameter	0.152 m
Pendulum velocity	4,76 m/s
Padding, material	Cell foam EPS 15 000 g/m^3
Padding, dimension (length, height, thickness)	0.220*0.190*0.100 m
Sled weight	13,0 kg

Instrumentation - Place the instruments (Table 12) in the positions as specified in section 5.

Table 12. Instrument positions and filters.

Measurement	**Requirement**	**Filter Class**
Pendulum velocity	4,76 m/s	Not specified
Peak force (mass x acce.)	4342-4676 N, from 14 to 17 ms	CFC 180 (300 Hz)
Sled peak acceleration	170-180 m/s^2, from 5 to 8 ms	CFC 60 (100 Hz)
Sled velocity, curve	See Table 13	From accelerometer and/or film data
T1 x-acceleration	See Table 15	CFC 180
Upper neck moments	See Table 15	CFC 600
Upper neck forces	See Table 15	CFC 1000

Data acquisition – The instrumentation signals are to be filtered according to Table 2 and sample at 10 000 Hz. Dummy motions should either be recorded at 500 f/s with either high-speed video or high-speed camera and digitized or the dummy si tioo be fitted devices which may record the T1 angular motions, the angle between the neck link and T1 as well as the angle between the head and the neck link.

Data analysis – Three coordinate systems are to be defined. Their x-axes are to be perpendicular to the z-axes and they are to be positive in the forward and upward direction respectively.

- The sled system is to move with the sled.
- The x-axis of the head accelerometer system is to be parallel with the head base, its center is to be located at the head CG and it rotates with the head.
- The x-axis of the T1 accelerometer system is to be horizontal, its center is to be located close to the C7-T1 joint pin and it is to rotate as the T1.

For the analysis of the head-neck kinematics, a two-link approach are to be used (Figure 2). The lower and upper pivot are to be located at the C7-T1 joint center and the C1-occipital interface joint center respectively. The neck link, which length is not to be constant, is to be defined as a line between these two points. The lower neck link angle (neck link relative T1 angle, θ_{T1}) is to be defined as the angle between the neck link and the T1 frame. The upper neck link angle (head relative neck link angle, $\varphi_{Neck\ Link}$) is to be defined as the angle between the head and the neck link.

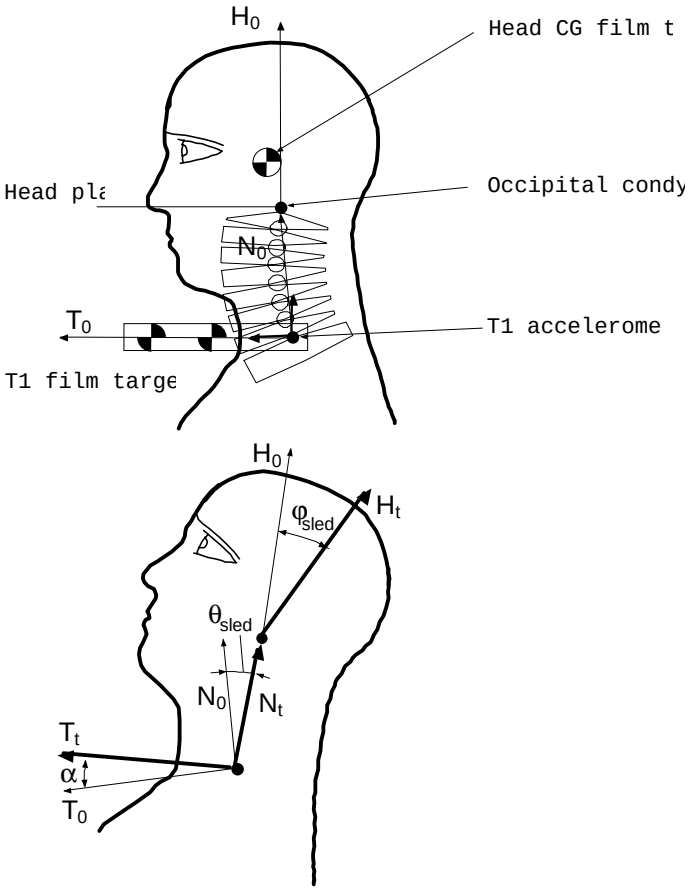

T1 angular displacement: α
Lower neck link angular disp.: $\theta_{T1} = \theta_{sled} - \alpha$
Head relative T1 angular disp.: $\varphi_{T1} = \varphi_{sled} - \alpha$
Upper neck link angular disp.: $\varphi_{Neck\ Link} = \varphi_{sled} - \theta_{sled}$

Figure 46**.** Schematic of the 2-pivot neck model (the lines represent angular positions at impact start and at time t for T=T1 vertebra, N=neck link and H=head).

Requirements - The BioRID II performance is acceptable when the measures defined in Table 2 fits inside the corridors specified in Table 3-5. The upper neck load cell data is to be defined in the future.

Table 13. Sled velocity corridor (m/s).

	Sled velocity	
Time (s)	Upper limit	Lower limit
0	0.20	-0.20
0.01	1.64	1.24
0.02	2.70	2.50
0.03	2.70	2.50
0.04	2.34	1.94
0.05	2.44	2.04
0.06	2.60	2.20
0.07	2.85	2.45
0.08	3.09	2.69
0.09	3.20	3.00
0.1	3.20	3.00
0.11	3.15	2.75
0.12	2.72	2.32
0.13	2.47	2.07
0.14	2.38	1.98
0.15	2.41	2.01
0.16	2.49	2.09
0.17	2.49	2.09
0.18	2.46	2.06
0.19	2.40	2.00
0.2	2.17	1.77
0.21	2.04	1.64
0.22	1.95	1.55
0.23	1.82	1.42
0.24	1.69	1.29

Table 14. Angular displacement response corridors (deg).

	T1		Head rel. T1		Neck link rel. T1		Head rel. Neck link	
Time (ms)	Upper limit	Lower limit	Upper limit	Lower limit	Upper limit	Lower limit	Upper limit	Lower limit
0.0	0.0	0.0	0.5	-0.5	0.5	-0.5	0.50	-0.50
10.0	-1.0	0.0	1.7	-0.3	1.5	-0.5	0.50	-0.50
20.0	-6.8	-4.8	6.8	3.8	6.0	3.5	1.00	0.00
30.0	-10.3	-8.3	8.4	5.4	3.5	0.5	5.80	3.80
40.0	-11.8	-9.8	4.5	1.5	-3.7	-7.7	9.40	7.10
50.0	-14.0	-12.0	0.0	-3.0	-8.5	-13.	10.50	7.40
60.0	-17.0	-15.0	-4.5	-7.0	-10.8	-15.3	10.00	6.40
70.0	-17.5	-15.5	-9.0	-13.0	-15.5	-20.0	8.50	4.50
80.0	-17.5	-15.5	-17.0	-22.0	-22.0	-26.5	6.20	2.60
90.0	-17.0	-15.0	-24.0	-29.0	-26.0	-30.5	3.60	0.60
100.0	-16.8	-14.8	-28.0	-33.0	-28.9	-33.4	2.00	-1.00
110.0	-17.3	-15.3	-29.0	-34.0	-29.5	-34.0	1.20	-1.80
120.0	-17.8	-15.8	-30.0	-35.0	-29.6	-34.1	0.80	-2.20
130.0	-18.0	-16.0	-30.5	-35.5	-29.5	-34.0	0.50	-2.50
140.0	-17.8	-15.8	-31.0	-36.0	-29.5	-34.0	0.30	-2.70
150.0	-16.9	-14.4	-31.0	-36.0	-29.6	-34.1	0.20	-2.80
160.0	-15.9	-13.4	-30.5	-35.5	-29.5	-34.0	0.15	-2.85
170.0	-14.4	-11.4	-30.0	-35.0	-29.4	-33.9	0.00	-3.00
180.0	-13.0	-10.0	-29.0	-34.0	-28.4	-32.9	-0.10	-3.10
190.0	-10.5	-7.5	-27.0	-33.0	-26.4	-30.9		
200.0	-8.0	-5.0	-25.0	-31.0	-23.0	-28.5		
210.0	-6.5	-3.5	-23.0	-29.0	-20.2	-25.7		
220.0	-5.5	-2.5	-21.0	-27.0	-17.7	-23.5		
230.0	-4.5	-1.5	-19.0	-25.0	-14.8	-20.8		
240.0	-3.0	0.0	-17.0	-23.0	-12.3	-18.4		
250.0					-9.7	-15.7		
260.0					-7.6	-13.7		
270.0					-5.3	-11.4		

Table 15. T1 x-acceleration corridor and neck load cell data corridors (to be defined).

	T1 x-acceleration (m/s^2)		Fx (N)		Fz (N)		My (Nm)	
Time(ms)	Upper limit	Lower limit						
0.0	0.0	0.0						
5.0	10.0	0.0						
10.0	35.0	-5.0						
12.5	60.0	-20.0						
15.0	0.0	-80.0						
20.0	-150.0	-210.0						
22.5	-185.0	-240.0						
25.0	-160.0	-240.0						
30.0	-40.0	-120.0						
35.0	70.0	-5.0						
37.5	85.0	15.0						
40.0	80.0	5.0						
42.5	20.0	-55.0						
45.0	0.0	-70.0						
50.0	30.0	-30.0						

8.2 Damper calibration test

This calibration test should only be carried out in special situations, e.g. when a new damper unit is assembled or when the results of the spine and torso evaluation test do not fulfil the requirements.

Method - The damper calibration test is carried out by loading the damper with a weight. A polyester rope (diameter 2 mm) should be attached to the damper (Figure 47). The polyester rope winding angle should approximately be 360 degrees. One end should be attached to a drop weight while the other end should be attached to a release mechanism. At test start, the release mechanism releases the rope and the weight drops 125 mm due to gravity and rotates the damper. The drop weight velocity should be calculated from video drop weight displacement data obtained by recording with high speed video (average calculation, window size of 9 rows, video recording rate at 250 frames/second), and plotted versus time.

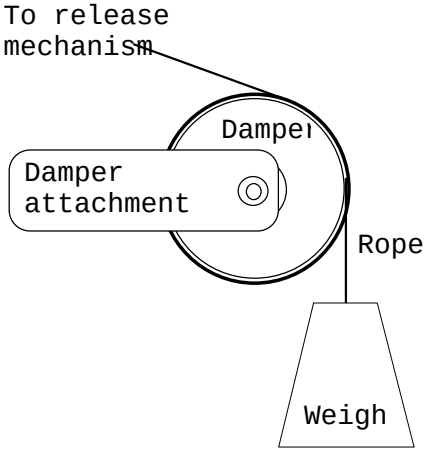

Figure 47. Damper calibration test arrangement.

Requirements - In order to perform acceptably, the damper velocity shall be within the limits defined in Table 16. If the damper does not perform within the specified range, the damper may be broken or manufactured with to large tolerances, the damper oil may be contaminated or the valve screw may not be in the proper position.

Table 16. Damper calibration test requirement limits.

Drop mass 9.0 kg			Drop mass 16.8 kg		
Time (ms)	Lower value (m/s)	Upper value (m/s)	Time (ms)	Lower value (m/s)	Upper value (m/s)
0	-0.10	0.00	0	-0.15	0.00
100	0.25	0.35	125	0.35	0.50
500	0.25	0.35	225	0.50	0.70
-	-	-	275	0.50	0.70

9 Future work

9.1 Redesign of neck rubber bumpers

The resistance to neck extension/flexion is controlled by muscle substitutes and rubber bumpers placed between adjacent vertebrae. In the BioRID I and BioRID II design, these rubber bumpers are of the same size and position, and have the same properties. The distances between two adjacent vertebrae in the initial neck posture are, however, somewhat smaller in the front than in the back. In order to get a correct initial neck posture, the anterior rubber bumpers have to be somewhat compressed while the posterior rubber bumpers are unloaded. Therefore, the frontal muscle substitute cables must be released prior to storage in order to prevent creep in the frontal rubber blocks.
To avoid this problem, the neck vertebrae, and the anterior and posterior neck bumpers need to be redesigned.
In order to reduce neck spine bumper creep due to constant load during storage, in-between adjacent neck vertebra resistance to flexion/extension should preferably be constituted by metal springs (similar to the thoracic and lumbar spine torsion pin design).

9.2 Increase durability

The silicon rubber used in the torso has a number of desirable properties. It is temperature insensitive, creep rate is low, the stiffness is low, it is easy to handle and to mould, its density is close to that of the human torso, it is resistive to chemicals and its adhesive ability to aluminum is acceptable. However, its resistance to tearing is too low.
To increase durability of the torso, different types of rubber may to be considered for future BioRID designs. Another alternative is to fit the torso with a durable skin. A larger water filled cavity in the abdomen of the torso in conjunction with a stiffer silicon may give the same resistance to bending while improving the durability. The design of the arm attachment and the pelvis interface may also be further improved.

9.3 Increase the pelvis rearward displacement in a rear impact

In the validation studies, it was concluded that the BioRID I and BioRID P3 pelvis rearward displacements were smaller than that of the average volunteer. In the BioRID I and P3 validation tests, the pre-impact seat panel displacements or the pre-impact contact pressure between the BioRID P3 pelvis and seatback resembled that of the volunteers. The smaller pelvis rearward displacements could have been caused by a too large pelvis aluminum structure, or too stiff pelvis flesh.
The pelvis design needs to be further accessed.

9.4 Evaluation of the range of motion

The BioRID spine range of motion was based on literature data. There are, however, no reliable range of motion data for the thoracic spine and lumbar and cervical range of motion data are from standing volunteers. Further evaluation of the effect of range of motion on BioRID kinematics, as well as volunteer range of motion data, is a necessity.

9.5 Evaluation of initial posture

The initial BioRID posture in a rear impact test influences the response. There is, however, a lack of reliable volunteer studies explaining proper initial sitting posture, spine shape, and back surface contour. These issues need to be further addressed.

9.6 Rebound velocity and forward kinematics

When comparing torso and head rebound velocities, the volunteer was slower than the BioRID I and BioRID P3. Further rebound and forward validation and dummy tuning is needed. This may call for thoracic spine joint kinematics partly controlled by dampers or call for an energy absorbing gel fitted inside the torso.

9.7 Head impact test

In order to control the stiffness of the back of the head a head impact test should be designed.

Method - The original Hybrid III head should be impacted posterially. The method used is in accordance with the Hybrid III forehead calibration method. 3-axial head accelerations are to be measured during the drop test. Filtering according to SAE J211.

10 List of BioRID prototypes

The following dummies have been developed, produced and tested at Chalmers/Autoliv/Linz/JARI. The listed prototypes have been modified throughout the validation studies:

BioRID P1 The torso was moulded in green silicon rubber and it had four horizontal slits. There was no water-filled cavity in the abdomen. A modified pedestrian HIII pelvis was used. The thoracic and lumbar vertebrae were made of aluminum. The neck was made of white plastic. The neck design was very similar to that of the RID-neck. Torsion pins Ø was 8 mm. Muscle substitutes acted between the T1 and head base. Two springs in parallel were mounted on an external rig (16.8 kN/m each). There was no damper.

ASTC-RID Similar to BioRID P1. No torsion pins in the thoracic and lumbar spine and no muscle substitutes were used.

BioRID P2 The torso was moulded in red silicon rubber (Wacker M4601 A+B with 50% AK35 silicon oil). The torso had a water-filled cavity in the abdomen. The torso had initially two horizontal slits, which later were closed. A modified HIII standard pelvis was used. All vertebrae were constructed of black POM plastic. The lumbar torsion pins were Ø 8 mm and the thoracic torsion pins were Ø 10 mm. An external muscle substitute package controlled the muscle substitute and consisted at first of a single damper but was later on a damper in parallel with a spring was added. The muscle substitutes were connected at T1 and the base of the head.

BioRID I (A, B and C)
Dummies delivered to partners within the consortium. The design was very similar to that of BioRID P2.

BioRID P3 The torso was moulded in red silicon rubber (Wacker RT623 A+B with 75% AK35 silicon oil). The torso was fitted with a water filled cavity but was without slits. A modified HIII standard pelvis was fitted to the dummy. All vertebrae were constructed of black POM plastic. The lumbar and thoracic spine torsion pins were Ø 8 mm.
The muscle substitute consisted of a single damper mounted in parallel with a flexor and an extensor spring. The spring and damper unit is placed inside the dummy. The muscle substitutes were connected at T3 and at the base of the head. The muscle substitute load was distributed to T1, T2 and T3.

BioRID II Dummies delivered to partners within the consortium. The design was very similar to that of BioRID P3.

11 Mathematical neck model

A new mathematical model consisting of a series of rigid bodies (representing the 7 cervical vertebrae and the upper most thoracic vertebrae, T1) connected by pin joints and supplemented by muscle substitutes was developed. The model was implemented using MADYMO 2D and restricted to motion in the sagittal plane. The motion of T1 was prescribed.

12 Mass properties of BioRID II

The masses of the different dummy parts are presented in Table 17.

Table 17. Mass of the BioRID II and human.

Body part:	BioRID II (kg)
Silicon torso incl. shoulder yoke and abdomen attachment exc. abdominal water	19.900
Abdominal water	2.060
Neck incl. muscle substitutes cables	0.916
Thoracic and lumbar spine, incl. pelvis interface	6.600
Head	4.522
Upper extremities	8.528
Lower extremities	23.315
Pelvis	10.700
Total	76.5

13 List of publications

Davidsson, J., Linder, A., Svensson, M.Y., Flogård, A., Håland, Y., Jakobsson, L., Lövsund, P., Wiklund, K. **BioRID - A New Biofidelic Rear Impact Dummy**. Proc. 1998 Int. IRCOBI Conf., Göteborg, Sweden, 1998b: pp. 377-390

Linder, A., Svensson, M.Y., Davidsson, J., Flogård, A., Håland, Y., Jakobsson, L., Lövsund, P., Wiklund, K. **The New Neck Design for the Rear-End Impact Dummy, BioRID I**. Proc of 42nd Annual AAAM Conf., Charlottesville, USA, 1998, pp. 179-192.

Linder, A., Svensson, M.Y., **An New Mathematical Neck Model for a Low Velocity Rear-End Impact Dummy: Evaluation of components Influencing Head Kinematics,** Proc. 1999 World Congress on Whiplash-Associated Disorders (WAD'99), Traffic Safety and Auto Engineering Stream; Vancouver, Canada, pp. 391-409.

Linder, A., Steffan, H., Lövsund, P., **Validation of the BioRID P3 against Volunteers and PMHS Data and Comparison to the Hybrid III in Low-Velocity Rear-End Impacts,** Proc. 43rd Annual AAAM Conf., Sitges, Spain, 1999, pp. 367-382.

Davidsson, J., Lövsund, P., Ono, K., Svensson, M.Y., **A Comparison between Volunteer, BioRID P3 and Hybrid III performance in Rear Impacts**. Proc. 1999 Int. IRCOBI Conf., Sitges, Spain, pp. 165-178.

Davidsson, J., Flogård, A., Lövsund, P., Svensson, M.Y., **BioRID P3 – Design and Performance Compared to Hybrid III and Volunteers in Rear Impacts at ΔV=7 km/h.** Proc. 43rd STAPP Car Conf., SanDiego, USA, 1999, SAE 99SC16, pp. 253-265.